Chapter 4 Influence of barium substitution on bioactivity, biocompatibility and physico-mechanical properties of bioactive glass

4.1 Introduction

Bone defects generally caused due to osteoporosis, infections, trauma, accidents and tumors in the human body. It necessitates the need for effective materials for regeneration of bone defects. Bioactive glasses are class of biomaterials which degrade in physiological solutions, forming a hydroxyl-carbonate apatite (HCA) layer on their surfaces which makes an intimate bond between the glass and living bone [31]. Mostly, the bioactive glass systems containing SiO_2–Na_2O–CaO–P_2O_5 have shown higher bioactivity in comparison to hydroxyapatite [2,3]. Since the discovery of 45S5 bioglass by Hench [1], there are significant research has been carried out with the substitution of various therapeutic ions like Sr^{2+}, Mg^{2+}, Co^{2+}, Cu^{2+}, Ti^{4+} and Zn^{2+} in the bioactive glass due to their regenerative properties not only osteogenesis but also angiogenesis [83][84][12][85][86][87]. It was reported that the strontium substituted bioactive glasses have shown enhanced biological properties in comparison to Sr-free bioglasses [48,55,88]. Moreover, the substitution of Sr bioactive glass stimulates the bone formation and reduces the resorption of bone [48][53][50]. Potential applications of Sr have been reported for treatment of osteoporosis and regaining of bone mass [58,89–91]. Further, it has been mentioned that strontium and other divalent cations with a similar charge-to-size ratio to calcium can be readily substituted in the lattice of hydroxyapatite [92][93][94]. Li et al., had reported that the large cations (like Sr^{2+}, Ba^{2+} and Pb^{2+}) would first replace Ca^{2+} at Ca(II) site in HA crystal structure [94]. It has been demonstrated that the substitution of Sr in the bioactive glass results in the mixed Sr-HA ($Sr_5Ca_5(PO_4)_6(OH)_2$) layer formation on the surface of the glass [47][57]. It was

also depicted that the addition of bigger Sr^{2+} ion in the HA matrix, the lattice parameter and crystal size increases [94]. The general formula for apatite is $[M_{10}\ (XO_4)_6Y_2]$, where M represents a bivalent cation, X represents a trivalent anion and Y represents a monovalent anion [15]. The divalent cations Mg^{2+}, Sr^{2+} and Ba^{2+} are similar charge of Ca^{2+} can easily be substituted in the lattice of hydroxyapatite. These divalent cations Mg^{2+}, Ca^{2+} and Sr^{2+} have shown significant effect on bone regeneration [84][55][48]. Hence, Ba^{2+} is one of the alkaline earth metal ions like Mg^{2+}, Ca^{2+} and Sr^{2+} and it can also show the bone regenerative properties. Moreover, Austin et al., confirmed that the barium distribution in teeth of human children have been found early life dietary transitions in primates [20]. It has been demonstrated in our previous work that barium containing bioactive glasses have shown the HCA layer formation in SBF [95]. Furthermore, earlier workers have demonstrated that the commercially available bone cement contains 10 % of barium as $BaSO_4$ to increase the radiopacity of the cement which is very useful during the radiographic imaging. Hence one can control the cement location during the clinical operations [43][44]. The ionic field strength of Ba^{2+} is less in comparison to Sr^{2+}, Ca^{2+} and Mg^{2+} in the glass network [96]. Consequently, the release of ions from the glass is relatively more which has less field strength and thus the HA layer formation would be much faster.

So, barium has many advantages to substitute in bioactive glass, but the role of barium on bioactivity and biological performances have been left to be studied. Moreover, Ba can also be substituted in the bioactive glass which would form the Ba-HA layer. It would further increase the lattice parameters and density of HA and it is expected to show a significant effect on bone regeneration. Moreover, there is less amount of research work earlier carried out with substitution of barium in bioactive glass. The addition of barium ion in bioactive glass increases its radiopacity in

comparison Mg, Ca, and Sr. However, it needs to be evaluated its cytotoxicity and biological behavior. The present work shows that the substitution of barium in the bioactive glass has a significant effect on bone formation and it would be potential material for dental and orthopaedic applications.

4.2 Materials and methods

4.2.1 Preparation of bioactive glasses

The chemicals were used in this experiment are analytical reagent grade (all from Loba Chemie, Mumbai, India) such as quartz, sodium carbonate, calcium carbonate, barium carbonate and ammonium dihydrogen orthophosphate as a source of SiO_2, Na_2O, CaO, BaO and P_2O_5 , respectively with a purity of 98- 99.9%. All were introduced in the form of their respective anhydrous state. The weighed batches were mixed thoroughly for 30 minutes and melted in platinum crucibles to get the desired bioactive glasses as given above in **Table 4.1**. The melting was carried out in an electric furnace at 1400 ± 5°C for 2 hours in air as furnace atmosphere and homogenized melts were poured on preheated aluminum sheet. The prepared glass samples were directly transferred to a regulated muffle furnace at 500 °C for annealing. Further, the glass samples were cooled gradually under a controlled rate of 10 °C per minute to room temperature after annealing for 1 hour at 500 °C. Further, the network connectivity (NC) of the glasses was calculated on the basis of general equation (4.1) [25,28] and given in **Table 4.1** assuming that SiO_2 form the network structure in the glass whereas, P_2O_5 remains in orthophosphate phase

$$NC = \frac{4 \text{ x } SiO_2 + 6 \text{ x } P_2O_5 - (2 \text{ x } CaO + 2 \text{ x } BaO + 2 \text{ x } Na_2O)}{SiO_2} \quad --(4.1)$$

Table 4.1 Chemical composition of the bioactive glasses (mole %) and network connectivity of the glasses.

Sample Name.	SiO_2	Na_2O	CaO	P_2O_5	BaO	NC
Ba-1	46.1	24.3	26.9	2.6	0.0	2.12
Ba-1	45.4	24.5	27.1	2.6	0.4	2.05
Ba-2	44.6	24.6	27.3	2.6	0.8	1.99
Ba-3	43.9	24.8	27.4	2.7	1.2	1.94
Ba-4	43.1	25.0	27.6	2.7	1.6	1.86

4.2.2 Heat-treatment of the bioactive glass samples

Sometimes the bioactive glasses are used as coating materials on metal implants and composites therefore they are subjected to heat-treatment. Hence it is better to know their crystalline phases present. The prepared bioactive glass samples were heat-treated in two-step system, firstly nucleation temperature for the formation of nuclei sites and after holding for the specific time, it was then further heated to reach the second selected crystal growth temperature after holding for the specific time. The samples were left to cool inside the muffle furnace to room temperature at a cooling rate of 10 ^{o}C per min.

4.2.3 U2OS cell line attachment and growth

The bioactive glasses were cut into thin discs using diamond blade cutter and autoclaved (sterilisation) before the test. The U2OS cells (5×10^4 cells/well) were seeded on the surface of the discs and incubated for 2 -7 days at 37°C, 5% CO_2. The growth of live cells images taken at the interface between culture plate and BG sample

at 2 and 7 day using a fluorescence microscope ((Nikon Eclipse 80i, Nikon, Japan). After incubation, the BG discs were taken out and rinsed three times with phosphate-buffered saline (PBS). The discs were dried at 37 °C for 24 h and subjected to AFM for morphology and height measurement. Further, the BG samples were sputter-coated a thin layer of gold prior to examination under SEM. The morphology and cell attachment on the surface of the bioactive glass were observed using SEM (Zeiss, EVO 18, Germany) and energy dispersive spectroscopy (EDS) (Oxford Instrument, X-act, Germany) for elemental analysis.

4.2.4 Atomic force microscopy (AFM) study

After culture of U2OS cell lines on the BG samples, the surface morphology of the bioactive glasses was studied using atomic force microscopy (AFM) (NTEGRA, NT-MDT, Russia) technique. Microscope was operated in the tapping mode regime and images were taken with a scan size of 25 μm × 25 μm and scan rate of 1.01 Hz. The images were taken under air atmosphere at room temperature.

4.2.5 Phagocytosis assay

Human macrophage was cultured from monocytes on test glass cover slips in complete medium from 5-7 days at 37 ^{o}C, 5% CO_2. The bioactive glass sample (25 mg/ml) was added to the macrophages and allowed to phagocytose for 24 h. The coverslips were washed, dried, fixed with ethanol and stained with Giemsa stain. Images of phagocytose macrophages were taken at room temperature. Phagocytosis analysis was performed by counting the phagocytic macrophages. The percentage of macrophages that were phagocytosed was calculated by dividing the number of macrophages that phagocytose the BG sample by the total number of macrophages counted multiplied by 100.

4.2.6 Opacity of the bioactive glass samples

In order to find out the radio opacity of the sample, Bulk glass samples (10 X 10 X 5 mm^3) were cut, ground and polished and they were optically clear. The samples were subjected to X-ray radiograph and the images were taken using dental X-ray machine (IRIX 70, Italy). The samples were irradiated at 70 kV and 8mA from a distance of 20 mm. and exposure time was 0.5 s.

4.2.7 *In vivo* animal studies

A total of 12 male Wistar rats (body weight **250-280** g) were used in the experiment and after obtaining permission from the Institutional Ethical Committee (no. Dean/2016/CAEC/45). Two groups of specimens (Bioglass® and Ba-3 samples) were implanted in rat femur bone. All the animals were anesthetized by intraperitoneal injection of 10% sodium pentobarbital at the rate of 4 mg per kg weight of the body [97]. The surgical skin was shaved and disinfected with povidone iodine. A longitudinal 2.0 cm incision was made along the femur bone. The subcutaneous tissue, muscles, and ligaments were dissected to expose the peripheral surface of the femur bone.

A 3 mm diameter defect was made in the femur end using a dental drill under continuous saline buffer irrigation as shown in **Figure 4.29**. Bioactive glass (Ba-0 and Ba-3) having particles size 0.4- 0.5 mm were implanted in to the drilled hole. After filling the hole, the ablated tissue and skin were repositioned and sutured layer by layer and these rats were transferred to cages. X-ray radiographic images were taken by Digital X-ray radiography instrument (Shimadzu RAD speed at 41 kV) at 0, 15, 30 and 45 days. The rats were sacrificed by intraperitoneal overdose of sodium pentobarbital after 60 days of implantation

4.2.8 *In vivo* blood analysis

After surgery, the blood was drawn at different time periods (0, 10, 30 and 60 days) for hematology analysis using retro-orbital blood sampling technique. The blood was collected for complete blood count (CBC) in anticoagulation tubes K3 EDTA (1.8 mg/ml). The CBC such as red blood cell count (RBC), white blood cells (WBC), hematocrit, hemoglobin, mean corpuscular hemoglobin (MCH), mean corpuscular volume (MCV), mean corpuscular hemoglobin concentration (MCHC) and Platelet were analyzed by Celltac E automatic analyzer (Tokyo, Japan).

4.3 Results and Discussion:

4.3.1 Differential thermal analysis curves of bioactive glasses

The thermal behavior curves of the bioactive glasses are shown in **Figure 4.1** and the results dictate that the incorporation of barium in the base bioactive glass reduced both the nucleation temperature from 614 to 542 ^{o}C and the crystallization temperature from 760 to 680 ^{o}C. Further, it could be observed that the higher amount of modifiers in the composition has facilitated in lowering T_g point and the viscosity of the glass melt [98]. On substitution of BaO for SiO_2 in the composition caused a shift of exothermic peaks to lower temperatures as compared to that of the base glass. Therefore, a lower energy is required to promote crystallization in the glass. This may be attributed due to the presence of larger Ba^{2+} ions in the system which increases interference in glass network. The modifiers occupied the interstitial positions in the glass structure and thereby weaken oxygen bond strength [99]. During the process of thermal treatment, the high concentration of barium in the glassy system creates more non-bridging oxygens which might have allowed an early nucleation by the nucleating agents like P_2O_5 in the glass composition.

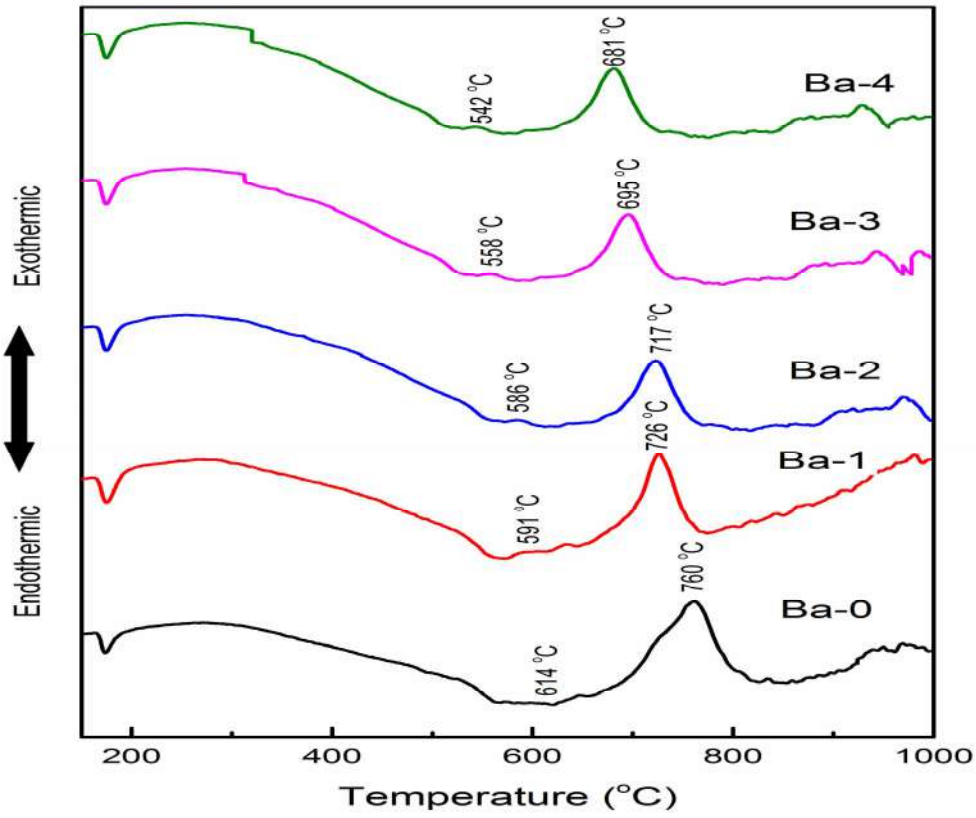

Figure 4.1 DTA curves of bioactive glass samples (Ba-0, Ba-1, Ba-2, Ba-3 and Ba-4).

4.3.2 Phase analysis of heat treated bioactive glasses

Figure 4.2 shows the XRD patterns of bioactive glass samples after controlled thermal treatment as given in **Table no.4.2**. All the bioactive glass samples show specific crystalline phases with small inconsistency in the intensity of the peaks depending on the composition and the heat-treatment schedule. The major diffraction sharp peak identified at $2\theta = 33.56°$ (hkl = 204) corresponds to $Na_2Ca_2Si_3O_9$ (Sodium calcium silicate) phase and the intensities of the diffraction peaks were matched with the standard PDF#: 22-1455. The earlier studies on sintered 45S5 bioactive glass had shown the same crystalline phase [100] [36]. It is well known that the Na_2O–CaO–P_2O_5–SiO_2 system has the tendency to form the sodium-calcium-silicate

phase as the main phase which was also confirmed earlier by earlier workers [101][102]. The secondary peak observed after barium substitution in the samples Ba-2, Ba-3 and Ba-4 at about 21.1° corresponding to Ca $(PO_3)_2$ (Calcium phosphate) PDF#: 50-0584. The intensity of the secondary peak increased with an increase in the concentration of barium oxide. It is well known that the addition of a few percent of P_2O_5 to silicate glass compositions promotes the volume nucleation and formation of glass–ceramic as indicated by Mastelaro [103]. It can be understood from XRD spectra that on addition of barium up to 1.6 mol% in the base bioactive glass system has not affected on the main crystalline phase within the specified heat treatment conditions.

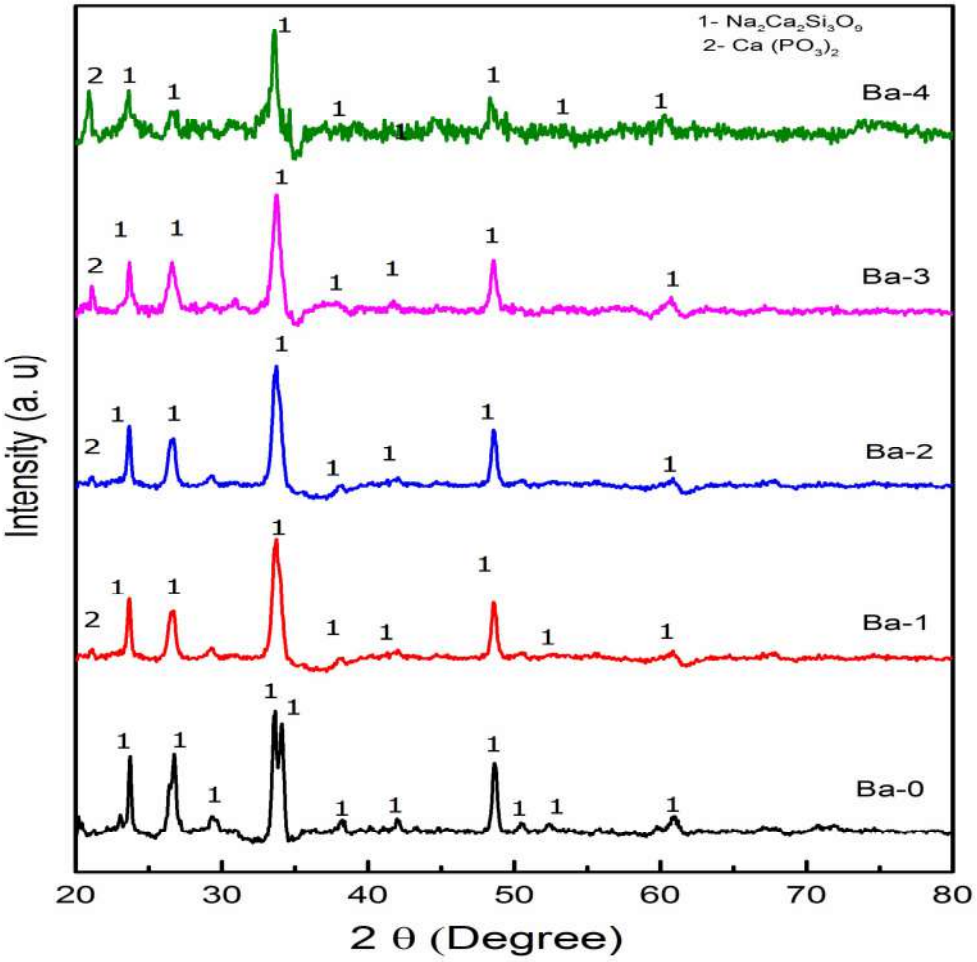

Figure 4.2 XRD pattern of the Ba-0, Ba-1, Ba-2, Ba-3 and Ba-4 bioactive glass samples sintered at different temperatures as given in Table 4.2.

Table 4.2 Heat treatment temperatures used for nucleation and crystal growth of bioactive glasses

Sample No	Nucleation temperature (°C)	Soaking time (hrs)	Crystallization temperature (°C)	Soaking time (hrs)
Ba-0	614	4	760	3
Ba-1	591	4	726	3
Ba-2	586	4	717	3
Ba-3	558	4	695	3
Ba-4	542	4	681	3

4.3.3 Structural analysis of bioactive glasses by FTIR spectrometry

Figure 4.3 shows the Fourier transform infrared (FTIR) transmittance spectra of the bioactive glass samples recorded in the frequency range of 400 – 4000 cm^{-1} on the FTIR spectrometer. The parent bioactive glass (Ba-0) revealed the sharp bands at about 450, 740, 1025, 1460 and 3420 cm^{-1}. The transmittance spectral bands of bioactive glasses have confirmed the main characteristic of SiO_4 tetrahedral silicate network and it is attributed due to the presence of SiO_2 as a major constituent. The resultant FTIR spectra at around 450 cm^{-1} is associated with a Si–O–Si symmetric bending mode and the band at 740 cm^{-1} corresponded to Si–O–Si symmetric stretching of non-bridging oxygen atoms between SiO_4 tetrahedral. The major broad band at about 1025 cm^{-1} can be attributed due to Si-O-Si asymmetric stretching. The minor sharp peak at 1420 cm^{-1} is attributed due to stretching mode of C-O vibration of CO_3 groups. The infrared frequencies and related functional groups were also reported earlier [104] in their bioglass ceramic systems.

The FTIR spectral bands of Ba-1, Ba-2, Ba-3 and Ba-4 samples have clearly shown the similar behavior like Ba-0 with small change in the band intensities (**Figure 4.3**). The barium substituted bioactive glasses up to 1.6 mol% did not show any major changes in the FTIR transmission spectral characteristics.

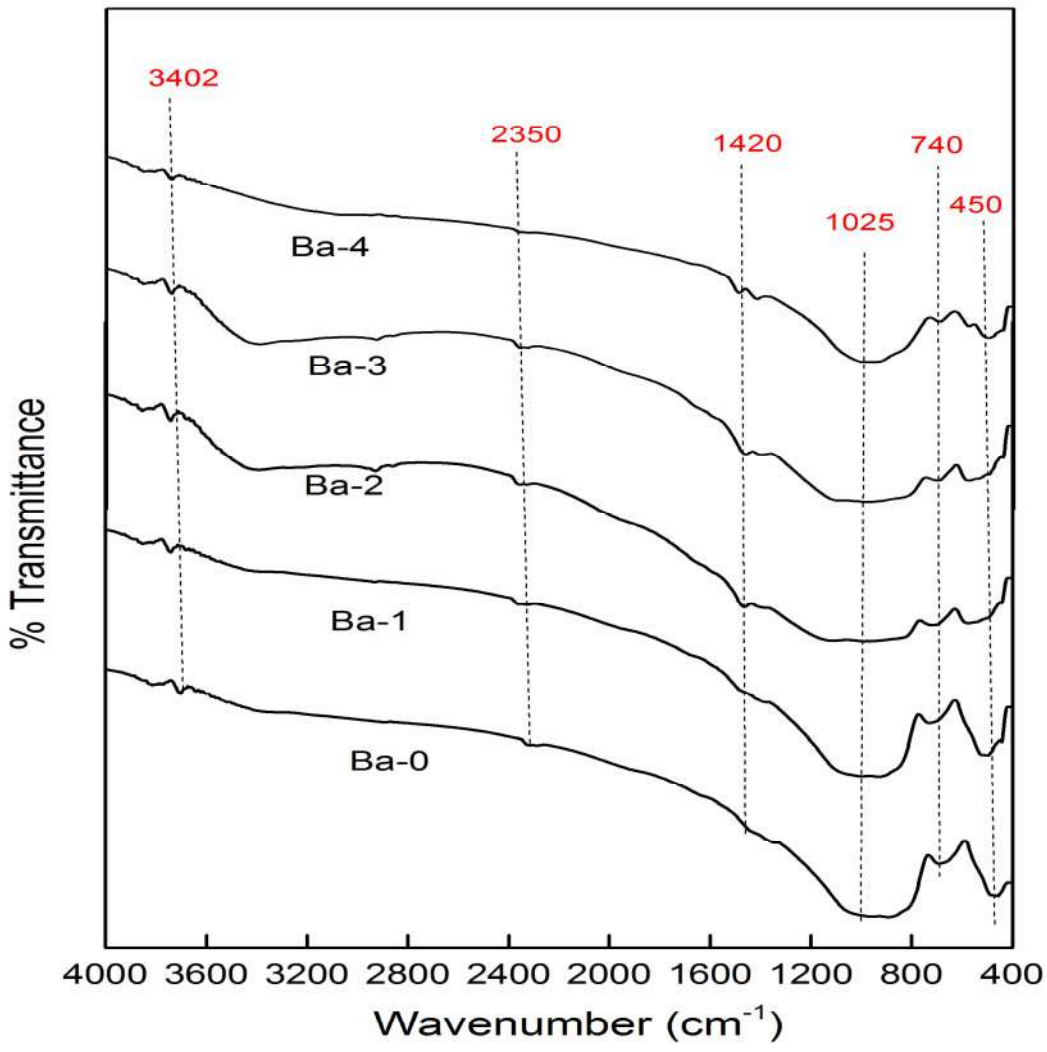

Figure 4.3 FTIR transmittance spectra of Ba-0, Ba-1, Ba-2, Ba-3 and Ba-4 bioactive glass samples

4.3.4 *In vitro* bioactivity and HCA formation in SBF

A. pH behavior of SBF after immersion of the samples

The pH behavior of the SBF solution after immersion of the bioactive glass samples can be clearly seen from **Figure 4.4**. The maximum pH values were recorded in all the samples within first 3 days as compared to the initial pH of the solution (pH =7.4). The pH values on third day were measured as pH= 9.38, 9.36, 9.44, 10.29 and 9.92 for the samples Ba-0, Ba-1, Ba-2, Ba-3 and Ba-4 respectively under physiological

conditions. The increase in pH can be explained as due to the fast release of Na^+ and Ca^{2+} ions through exchange with H^+ or H_3O^+ ions into the solution. The H^+ ions being replaced with cations thereby resulted in an increase in hydroxyl concentration of the solution which led to attack in silicate glass network and formation of silanols. The dissolution rate as well as pH increment decreased after 4 days due to the decrease of Na^+ and Ca^{2+} ionic concentration from sample surface. The reason for this decrease in the pH can be considered due to the precipitation of Ca^{2+} ions from the solution to form calcium phosphates and carbonates, Greenspan and others showed the same behavior and changes in pH after in vitro dissolution of the samples for various time periods[37][30][105].

Moreover, the sample numbers Ba-3 and Ba-4 with higher barium content were found to posses the highest rate of dissolution and hence the maximum pH values were recorded as compared with base bioactive glass sample (Ba-0). Previously it was demonstrated by Koenderink et al that the order of reactivity of the glasses with the alkaline earth ions Ba>>Sr>Ca≈Mg in water [106]. Furthermore, the substitution of BaO for SiO decreases the glass network connectivity (NC) and the release of ions can be much easier [107] (**Table 4.1**). Therefore, the incorporation of barium oxide into 45S5 bioglass® has resulted in an increase in the pH of SBF. The formation of apatite in SBF is strongly pH dependent and the most interesting aspect is that the cross linking of the collagen chains and the subsequent precipitation of hydroxy apatite on bone formation are pH dependent. Hence it requires a high pH at the bone formation site. The barium substituted bioactive glasses have been proposed as potential materials for bone tissue regeneration.

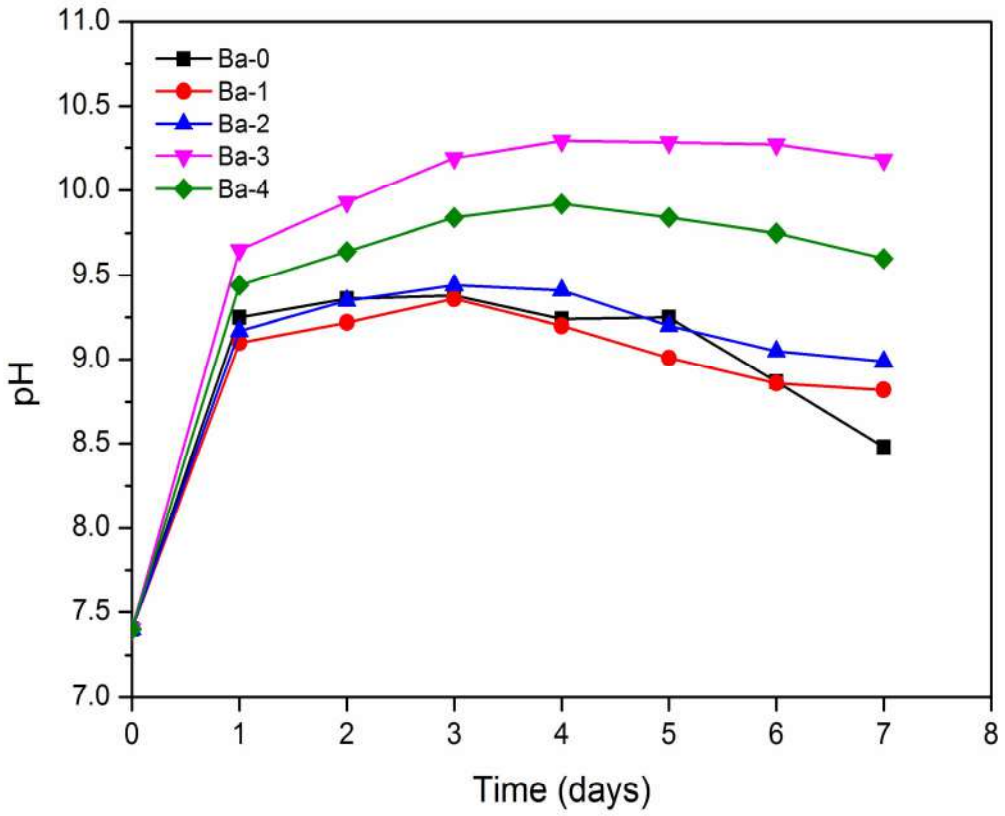

Figure 4.4 pH behavior of SBF after immersion of the Ba-0, Ba-1, Ba-2, Ba-3 and Ba-4 bioactive glass samples for 7 days

B. *In vitro* bioactivity of bioactive glasses by FTIR spectrometry

Figures (4.5 – 4.9) show the FTIR transmittance spectral bands of the bioactive glasses before and after immersion in SBF for different time periods such as 1, 3, 7, 14, and 30 days. In general, it is well known that a decrease in the intensity of transmittance bands indicates an increase in molecular concentration of species formed at surface of the bioactive glass treated with SBF solution with an increase in soaking time. The present results obtained by FTIR spectrometry were also in good agreement with the earlier studies made by previous workers [37][108] [109].

Figure 4.5 shows the infrared spectral bands of Ba-0 sample before and after immersion in SBF. The new bands were found to appear after 1 day immersion in

SBF at wavenumbers 578 and 661 cm^{-1} which correspond to (phosphate) P-O bending. The bands corresponding to the frequencies of 883 and 1602 cm^{-1} are associated with (carbonate) C-O stretching mode and a broad band at about 3380cm^{-1} can be assigned due to the presence of (hydroxyl) O–H groups on the surface. The prolonged period of the sample in SBF shows the similar behavior with small decrease in the intensities of the bands which resulted favorably due to the formation of hydroxyl carbonate apatite (HCA) layer.

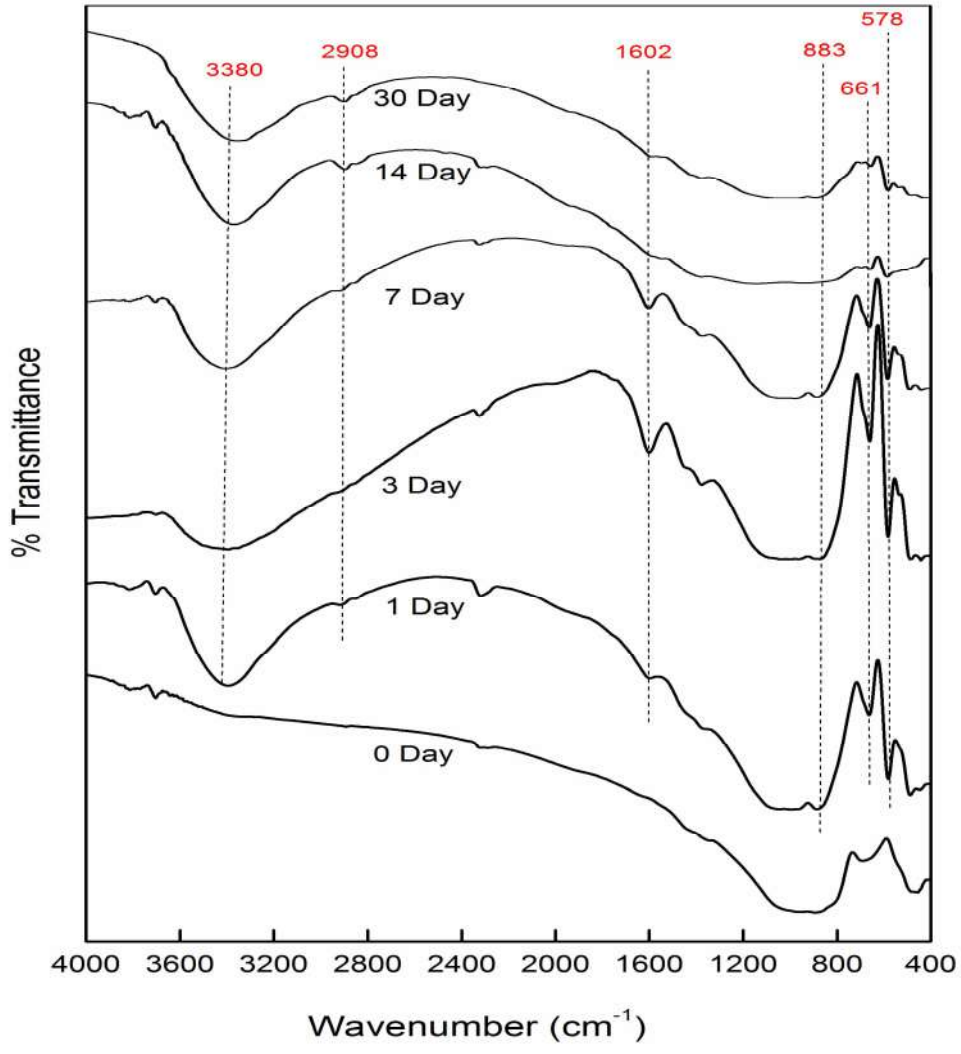

Figure 4.5 FTIR transmittance spectra of the Ba-0 bioactive glass sample before and after immersion in SBF for 1, 3, 7, 14, and 30 days

Figure 4.6 shows the IR spectral bands of Ba-1 sample before and after treatment with SBF. The new bands were revealed after 1 day treatment with SBF at 586 and 659 cm^{-1} which are attributed due to (phosphate) P-O bending. The bands at 879 and 1618 cm^{-1} are assigned due to (carbonate) C-O stretching mode of vibration and the band at about 3414 cm^{-1} was due to the presence of (hydroxyl) O–H groups on the surface. The prolonged period in SBF shows the similar behavior with small decrease in the intensities of the bands which resulted due to the formation of HCA layer on the sample surface.

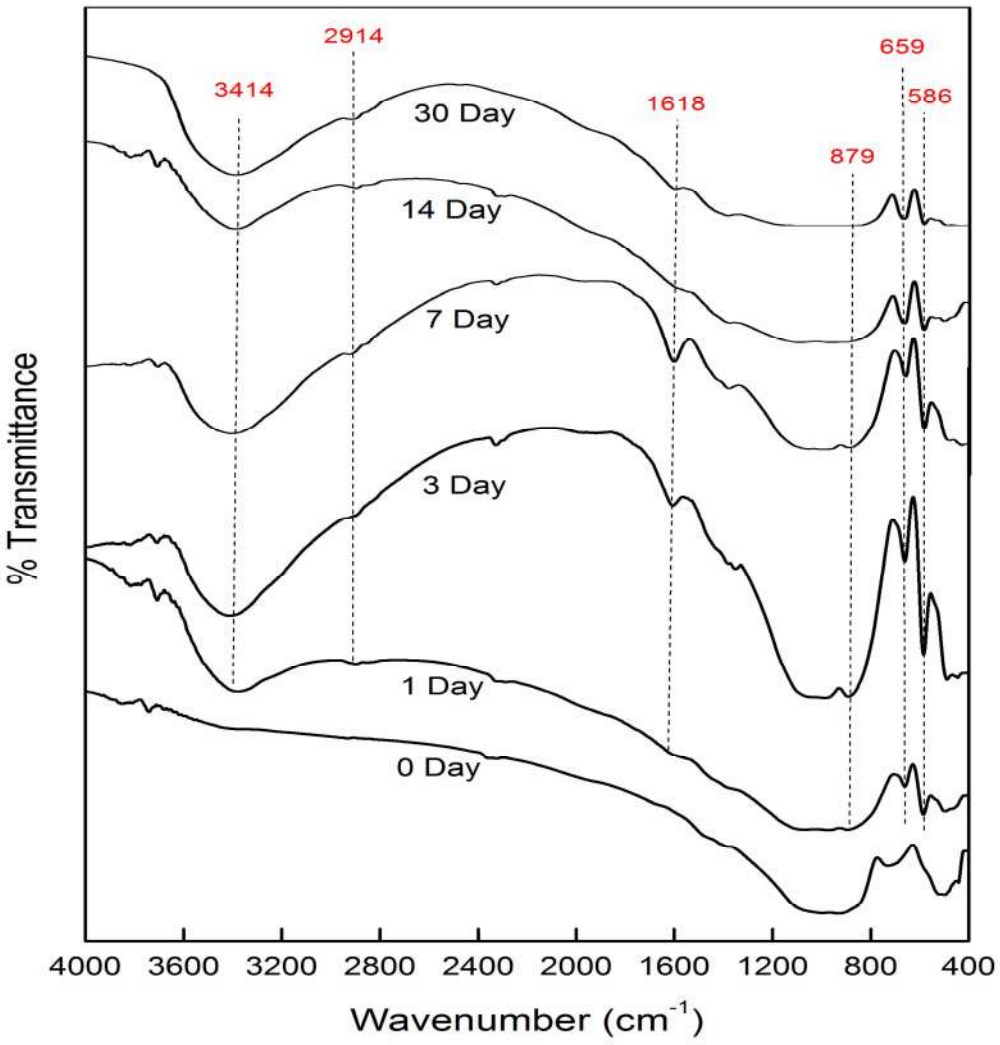

Figure 4.6 FTIR transmittance spectra of the Ba-1 bioactive glass sample before and after immersion in SBF for 1, 3, 7, 14, and 30 days.

Figure 4.7 shows the bands of Ba-2 sample before and after immersion in SBF. The new bands appeared after immersion in SBF for 1 day at 551 and 632 cm^{-1} which are related to (phosphate) P-O bending. The bands at 872 and 1573 cm^{-1} correspond to (carbonate) C-O stretching mode and the band at about 3359 cm^{-1} is assigned as usual due to formation of (hydroxyl) O–H groups on the surface of the sample. The prolonged period of the treatment of sample in SBF shows the like behavior with small decrease in the intensities of the bands which resulted in hydroxyl carbonated apatite layer formation on the sample.

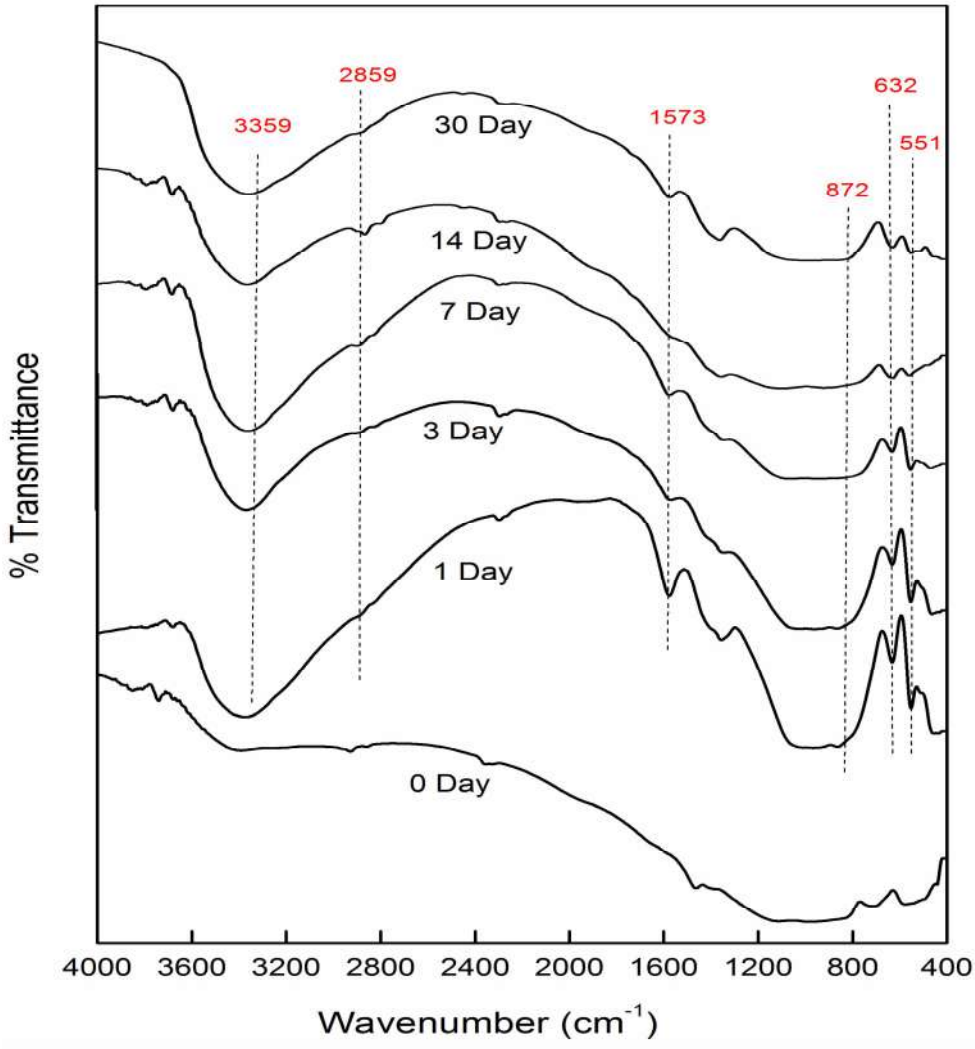

Figure 4.7 FTIR transmittance spectra of the Ba-2 bioactive glass sample before and after immersion in SBF for 1, 3, 7, 14, and 30 days

Figure 4.8 shows the bands of Ba-3 sample before and after immersion in SBF. The new bands recorded after immersion in SBF for 1 day at 567 and 640 cm^{-1} and they are associated with (phosphate) P-O bending. The bands at 956 and 1596 cm^{-1} correspond to (carbonate) C-O stretching mode and the band at about 3402 cm^{-1} is attributed due to the presence of (hydroxyl) O–H groups on the surface of the bioactive glass sample. The prolonged period of the sample in SBF shows the similar behavior with small decrease in the intensities of the bands and this dictated for the hydroxyl carbonated apatite layer formation.

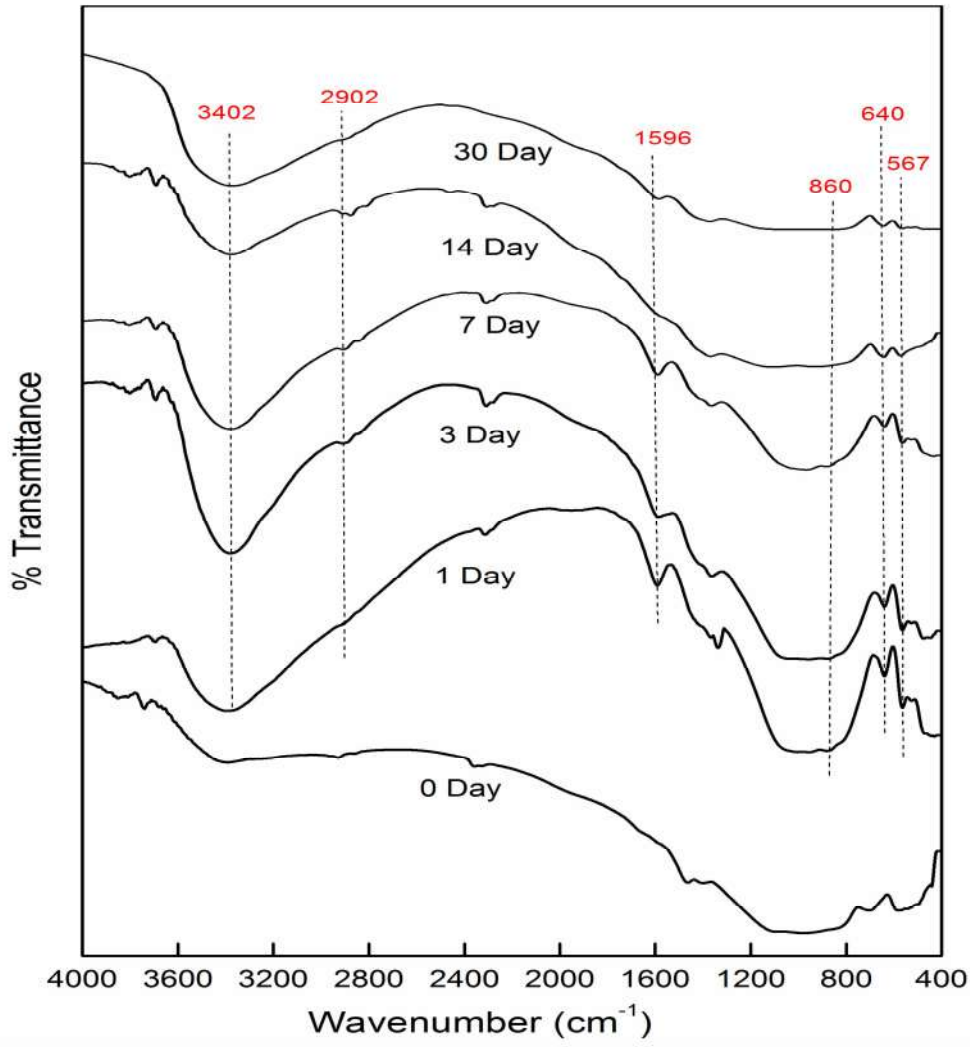

Figure 4.8 FTIR transmittance spectra of the Ba-3 bioactive glass sample before and after immersion in SBF for 1, 3, 7, 14, and 30 days

Figure 4.9 shows the bands of Ba-4 sample before and after it was soaked in SBF. The new bands were recorded after 1 day soaking in SBF at 535 and 616 cm^{-1} which are associated with (phosphate) P-O bending. The FTIR bands obtained at 844 and 1562 cm^{-1} correspond to (carbonate) C-O stretching mode of vibration and the band at about 3350 cm^{-1} was attributed due to (hydroxyl) O–H groups on the surface of the sample. The prolonged period of the sample in SBF shows the similar behavior with small decrease in the intensities of the bands which favored for the formation of hydroxyl carbonated apatite layer. It may be noted from FTIR spectra as given in **Figures (4.6-4.9)** that the barium substitution in base bioactive glass at the cost of silica did not affect in apatite formation.

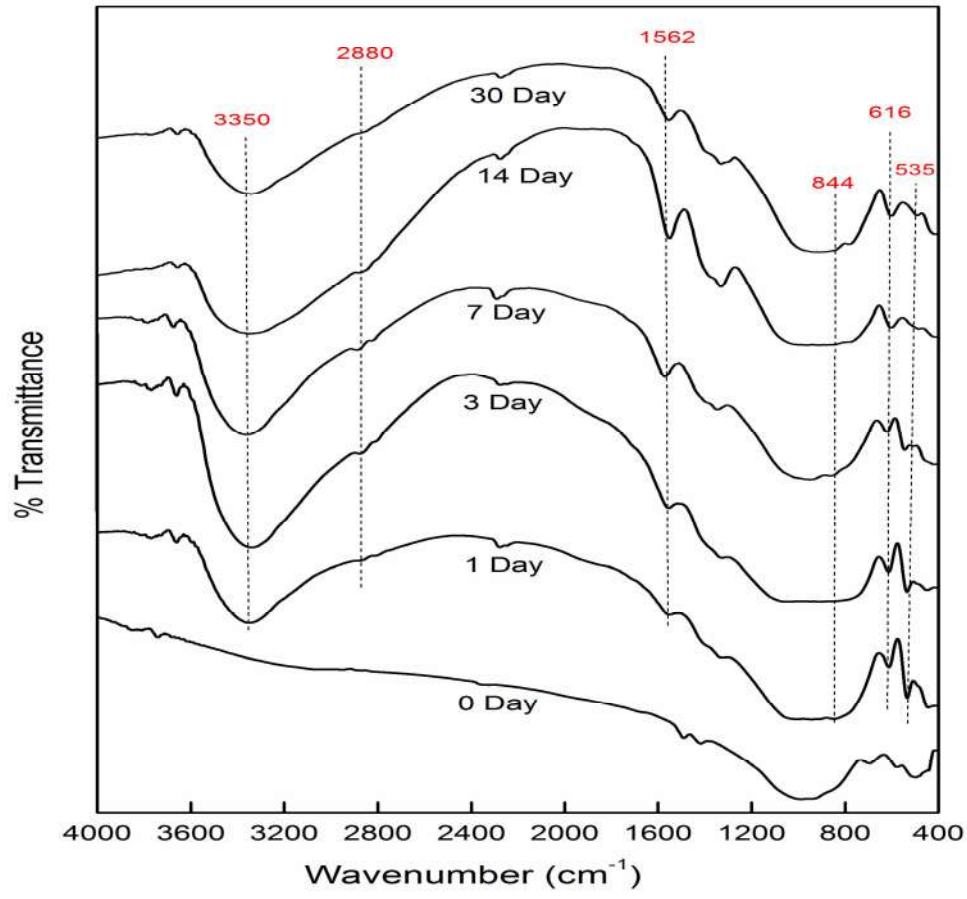

Figure 4.9 FTIR transmittance spectra of the Ba-4 bioactive glass sample before and after immersion in SBF for 1, 3, 7, 14, and 30 days

C. Surface morphology of bioactive glass samples by SEM

Figures (10- 11) show surface morphology of all the bioactive glass samples (Ba-1, Ba-2, Ba-3 and Ba-4) by their SEM images before and after the immersion in the simulated body fluid for 14 days at 37 ^{o}C. The changes in the surfaces of the bioactive glass samples after immersion in SBF can be easily differentiated from the SEM images (**Figure 11 A-D**) with respect to the images of the samples before SBF treatment as presented in **Fig 10 A-D**. The micrographs as given in Fig. 12 exhibit the layer of polycrystalline ball-like particles formed on surface of the samples after SBF treatment, which encourages the growth of the same crystallinity [38]. The developed crystals on the surface of the bioactive glasses is assumed to be hydroxy carbonate apatite, since the HCA layer is round in shape and varies in intensity from one sample to another [31]. It is interesting to note that with the increase in barium concentration the extent of HCA crystals was found to increase progressively as evident from the SEM pictures of the samples presented in figure 12 (A-D) . It is worth to note that the barium substituted bioactive glasses can also produce HCA like structure on their surfaces in SBF in vitro. The formation of apatite layer is also supported by the results obtained from XRD and FTIR spectrometry after immersion of the bioactive glass samples in SBF.

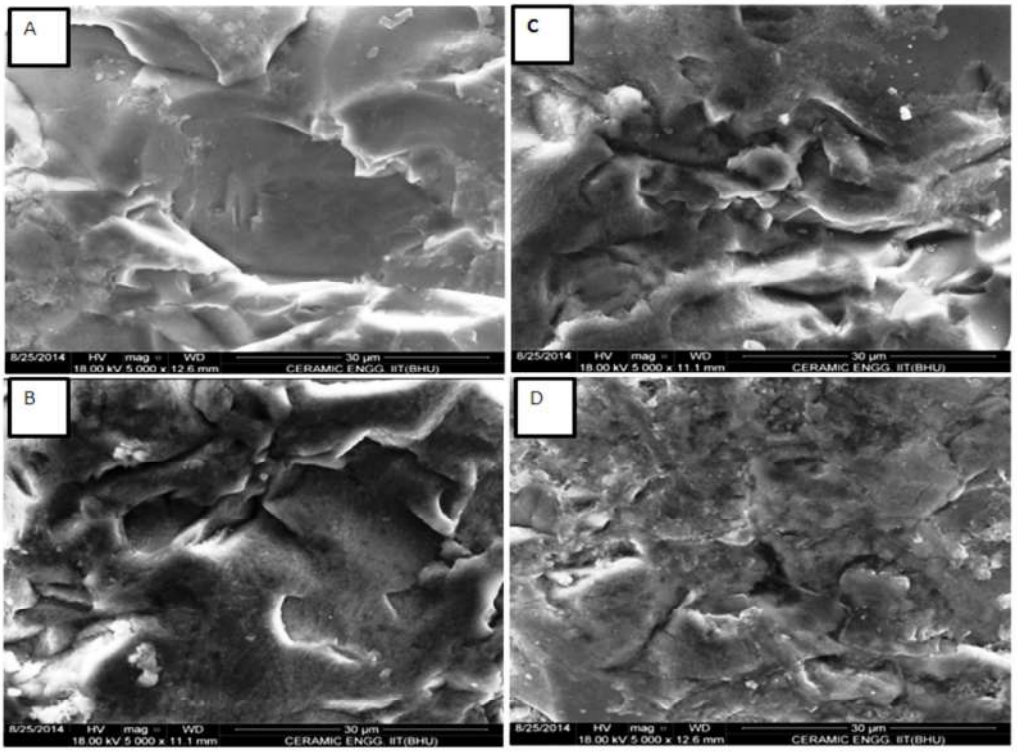

Figure 4.10 (A-D) Scanning electron micrographs of the Ba-1, Ba-2 Ba-3 and Ba-4 bioactive glasses before immersion in SBF, respectively

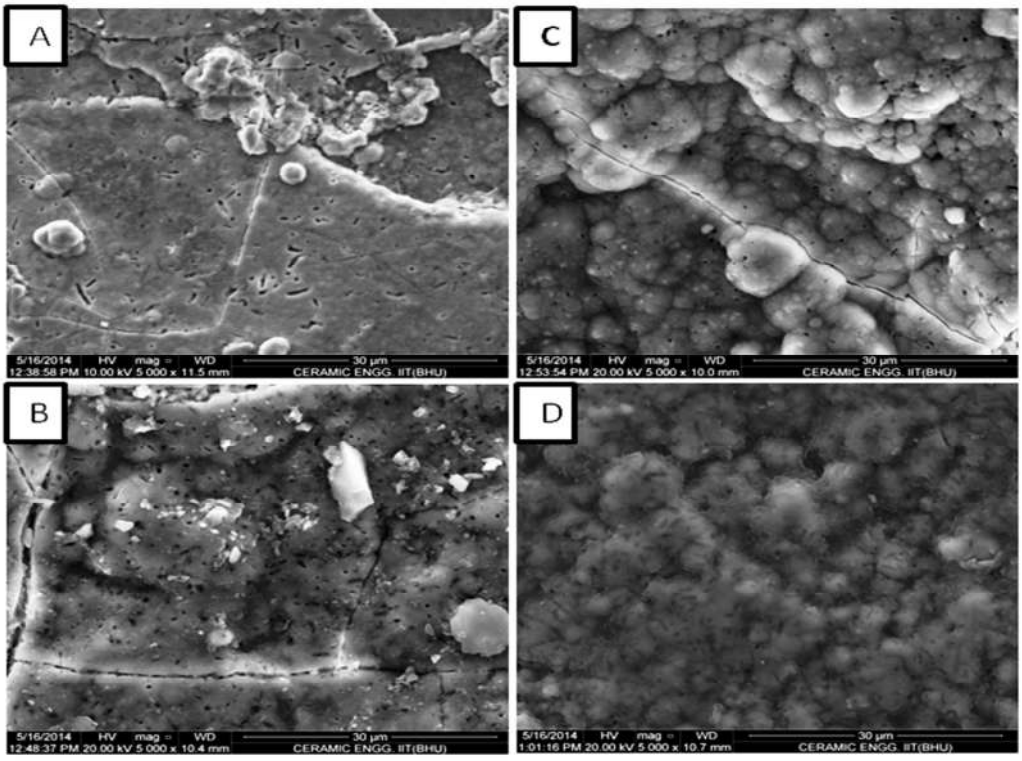

Figure 4.11 (A-D) Scanning electron micrographs of the Ba-1, Ba-2 Ba-3 and Ba-4 bioactive glasses after immersion in SBF for 14 days, respectively

D. *In vitro* bioactivity of the bioactive glasses by X-ray diffractometry

Figure 4.12 shows the XRD pattern of the bioactive glass samples (Ba-0, Ba-1, Ba-2, Ba-3 and Ba-4) before and after immersion in SBF for 14 days under physiological condition. It is evident from the XRD data that the prepared bioactive glasses had shown homogeneity and amorphous state which indicative of the internal disorder and glassy nature before immersion in SBF. Notably, the amorphous scattering of a broad hump at ≈32° found in the base bioactive glass and the broad peak became more intense as the concentration of BaO increases in the glasses. This difference might be due to the effect of barium contracting the silicate network.

In general, the bioactivity of the sample is associated with the ability of hydroxy carbonate apatite (HCA) layer formation on their surface in SBF. The **Figure 4.12** also contains the XRD pattern of hydroxyapatite (HA) powder [36] for comparison of crystalline HA layer formation on the surface of the SBF treated bioactive glass samples. In view of this, the XRD patterns of the SBF treated samples have clearly shown the formation of crystalline HA on their surfaces after immersion in SBF for 14 days as shown in **Figure 4.12**. The XRD peak located at 2θ at around 31.8° corresponds to (211) crystalline phase regarded as hydroxyapatite [Ca_{10} $(PO_4)_6$ $(OH)_2$] and the diffraction peaks were matched with the standard PDF#: 74-0565 [37-38]. However, all the samples after immersion in SBF showed the calcite phase at 2θ at around 29.46° (PDF No. 85-1108) in addition to HA, whereas the Ba-0 sample has shown the calcite as the major phase. In the Ba-0 bioactive glass sample formation of calcite phase has hindered the formation of HA layer on the surface of the bioactive glass. Tulyaganov et al [39] had also observed that a decreasing intensity of HA peaks was accompanied by

the formation of relatively high intensity calcium carbonate (calcite) peaks, which suggested that the early deposition of HA layer was gradually suppressed by freshly precipitated calcite in 45S5 Bioglass®. Kansal et al. [40] had also shown the calcite formation in all their SBF treated glasses including 45S5 Bioglass® which masked the precipitation of crystalline HA layer on the surface of the samples. The present trends are well supported by earlier results [39-40]. Further, it is mentioned herewith that calcite is a biodegradable material which exhibits strong bonding to the bone. It is interesting to note as evident from XRD patterns of bioactive glasses that an increase in barium content in the samples has decreased the tendency of calcite formation and simultaneously resulted in the formation of crystalline HA layer on the surface of the bioactive glasses as shown in **Figure 4.13**.

The investigation was carried out here for the qualitative characterization of HCA phase identification in the barium substituted bioactive glasses. The diffraction pattern of all the tested samples Ba-0, Ba-1, Ba-2, Ba-3 and Ba-4 demonstrated the same crystalline phases as hydroxyapatite and calcite. The intensity of the diffraction pattern is the only difference which was observed and this difference is attributed due to the different amounts of phases formed on each sample.

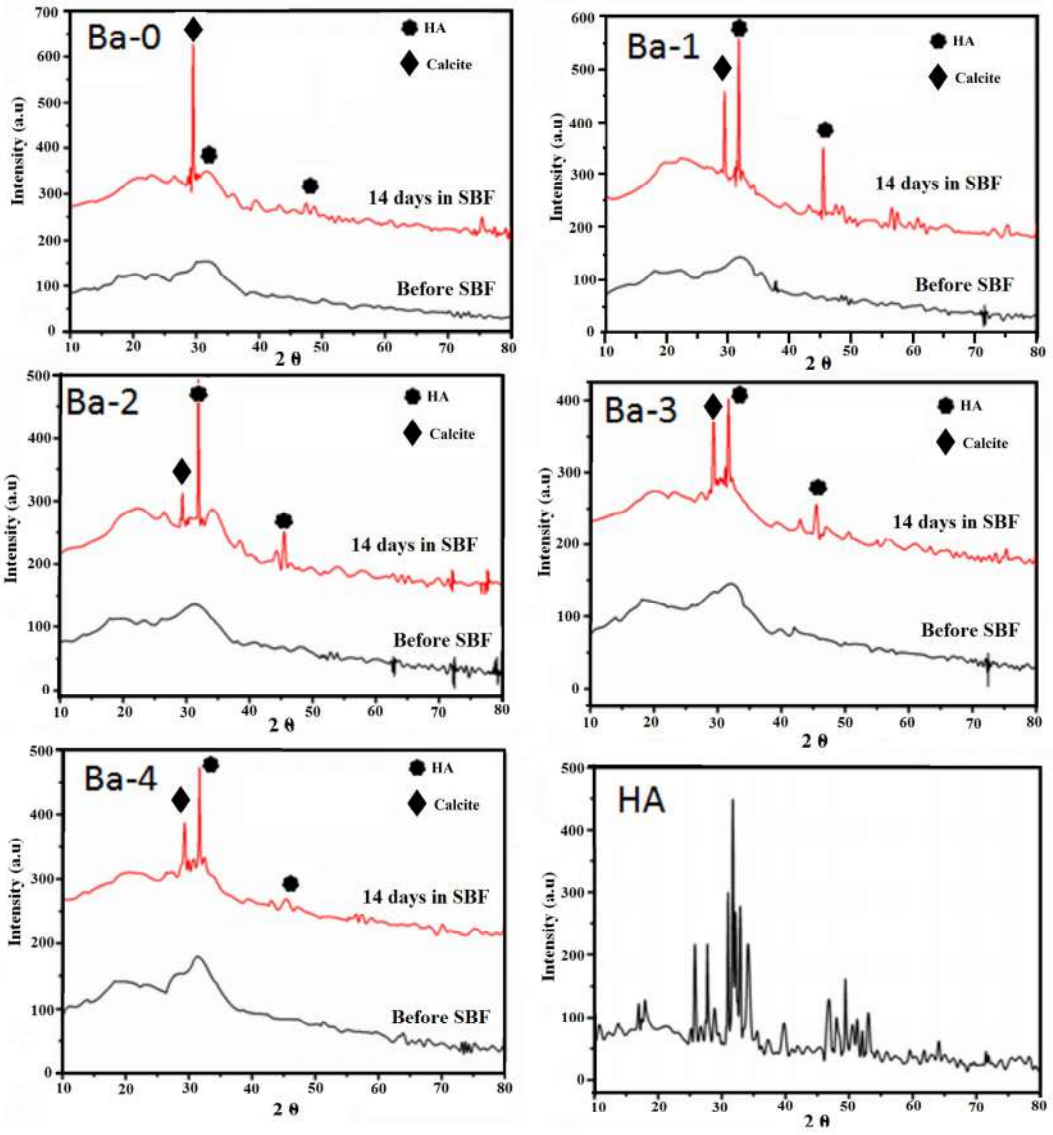

Figure 4.12 XRD pattern of Ba-0, Ba-1, Ba-2, Ba-3 and Ba-4 bioactive glass samples before and after SBF treatment for 14 days and Hydroxyapatite

Further, it was observed that the intensity of the peak (211) has varied with each other and this could be associated with the amount of phase formed in each sample as shown in **Figure 4.1**. Moreover, the (211) reflection corresponds to strongest HA peak, Hence, the HA crystallite size was calculated using Debye Scherrer formula as given in equation (4.2) [36,94] and it was found to be 2.96 nm, 38.46 nm, 25.23nm, 18.04 nm and 21.19 nm for Ba-0, Ba-1, Ba-2, Ba-3 and Ba-4, respectively. This significant development in HA is due to the substitution of baria for silica, which

lowers the glass NC and thus creating more number of non-bridging oxygens (NBOs). The low NC glasses release the alkali and alkaline earth ions much easier and faster. Hence, the surface becomes rich in silanols (Si-OH groups). Subsequently, this layer plays an important role in adsorption of calcium and phosphate ions from the solution. Therefore, the precipitation of Ca-P layer would be much faster. Possibly, this might have resulted in significant growth of HA crystallinity in barium contained bioactive glasses

$$D = \frac{0.9\lambda}{\beta \cos \theta} \qquad ---------(4.2)$$

Where, D is the crystallite size, β is the full width at half maxima (FWHM) excluding instrumental broadening, λ is the wave length of X-ray diffraction and θ is the Bragg angle.

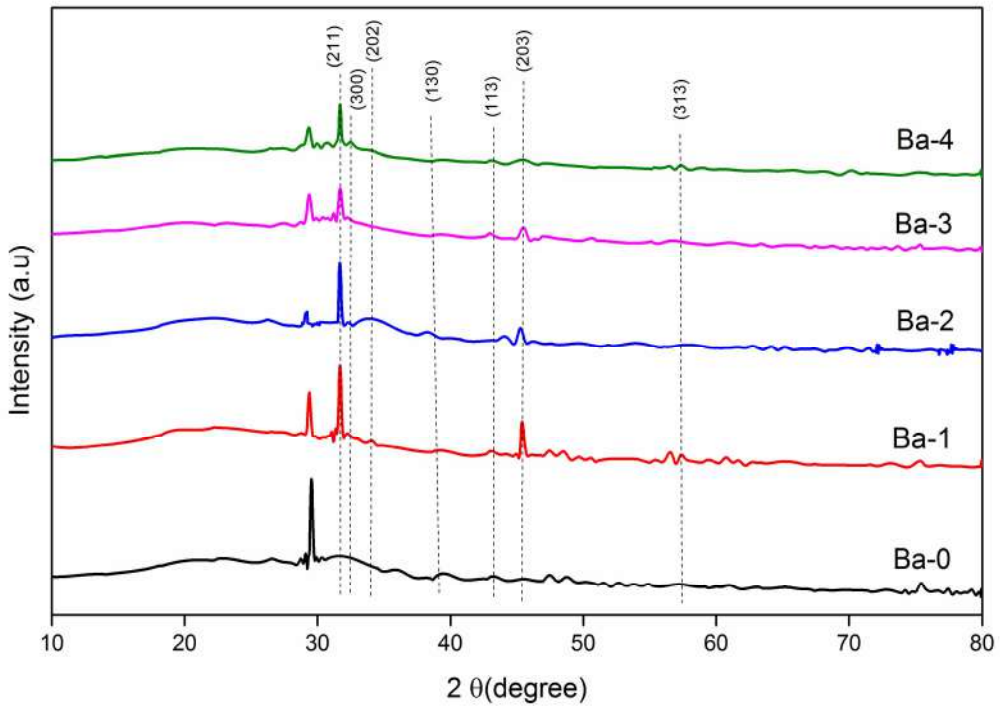

Figure 4.13 XRD pattern of Ba-0, Ba-1, Ba-2, Ba-3 and Ba-4 bioactive glass samples after immersion in SBF for 14 days

E. Thickness of HCA layer formation on bioactive glass blocks

In order to check the surface reactivity and HCA layer formation on the bioactive glasses (Ba-0, Ba-3 and Ba-4) in SBF, the bulk glass samples (10 X 10 X 5 mm^3) were immersed in SBF for 14 days and they were cut into cross section using diamond cutting machine and examined under the SEM & EDS. It was observed that the phase separation of the samples can be distinguished from the SEM images as shown in **Figure 4.14 (A-C)**. The thickness of the reacted layer was approximately estimated from the SEM images [12]. Three distinct areas were selected to measure the thickness and the mean was found to be 50.71 μm, 59.54 μm and 94.79 μm for Ba-0, Ba-3 and Ba-4 samples respectively. It was found that the thickness of the reacted layer has increased with increasing barium concentration in the BG. This indicates that the substitution of barium in the BG increases its reactivity in SBF in comparison to barium free (Ba-0) glass sample. Further, the reacted layer was analyzed for the elemental distribution of samples Ba-0 and Ba-4 using EDS as shown in **Figure 4.14 (D & E)** (**Oxford Instrument, USA**). It can be seen clearly that the reacted layer was marked (approx 100 μm) for classification of elemental distribution. The Ba-0 sample shows the initial layer approx 20 μm thicknesses of Ca and P rich depositions. Whereas, in Ba-4, the initial area approx 35 μm was found to be rich in Ca and P ions and poor in Si and Na ions deposition. This is showing the initial layer of HA layer and silica rich layer (Si-OH) in the middle where as the Na ions were almost leached out from the sample surface. Hence, the phenomenon has further strengthened the high HA layer formation. Hence, results suggest that the addition of barium not only increased the glass reactivity but also increased the HA layer formation significantly. Further, this is in good support with the earlier investigation carried out by Koenderink et al, who had

demonstrated the order of reactivity of the glasses with the alkaline earth ions Ba>>Sr>Ca≈Mg in water [106].

Further, it is interesting to note that the Ba^{2+} ions are also present on the surface of the reacted layer. It is important to discuss here that the earlier workers [110][47] had demonstrated that the substitution of Sr^{2+} ion in bioactive glass increases the ions dissolution rates and HA layer formation more rapidly. Moreover, Donnel et al [57] showed that the Sr^{2+} can be partially substituted in the lattice of HA due to the similar charge to size ratio to Ca^{2+} and reported the mixed Sr-HA [$Sr_5Ca_5(PO_4)_6(OH)_2$] layer formation. Therefore, the unit cell volume, lattice parameters and density of Sr-HA were found to increase linearly with Sr substitution due to the larger Sr^{2+} ion (ionic radii 1.13 Å) than Ca (0.99 Å) [57]. Further, it was reported that the large cations (like Sr^{2+}, Ba^{2+} and Pb^{2+}) would first replace Ca^{2+} at Ca(II) site in HA crystal structure [94][57]. Moreover, Mathew et al. [46] had substituted larger Ba^{2+} ion in the mineral fluoroapatite ($Ca_{10}(PO_4)_6F_2$) crystal structure and they have shown the formation of $Ba_{10}(PO_4)_6F_2$ crystal structure by single –crystal X-ray diffraction. In the present investigation, it is possible that Ba^{2+} ion might have partially substituted in the HA crystal lattice to form the mixed Ca-Ba-HA ($Ba_5Ca_5(PO_4)_6(OH)_2$) layer on the surface of the glasses. It is evident from EDS spectra that Ba^{2+} ions are present in the newly formed layer after SBF immersion (**Figure 4.14 E**). Since, Ba^{2+} ion (1.35 Å) is still heavier and larger than Ca^{2+} and Sr^{2+} ions thus the precipitation of Ba^{2+} ions from the SBF can be quite faster than Ca^{2+} and Sr^{2+}, hence the formation of HCA layer could be sooner and larger. It is in good agreement with the XRD results of the Ba-contained samples after immersion in SBF which exhibited the enhanced HCA layer formation and crystal size (**Figure 4.13)**. Consequently, the lattice parameter, unit cell volume and density might further increase with the substitution of bigger Ba^{2+} ions in the HA

crystal lattice. Therefore, the denser bone (Ba-HA) would be developed and it would have a better advantage over that of HA, as it may be used for the treatment of osteoporotic bone.

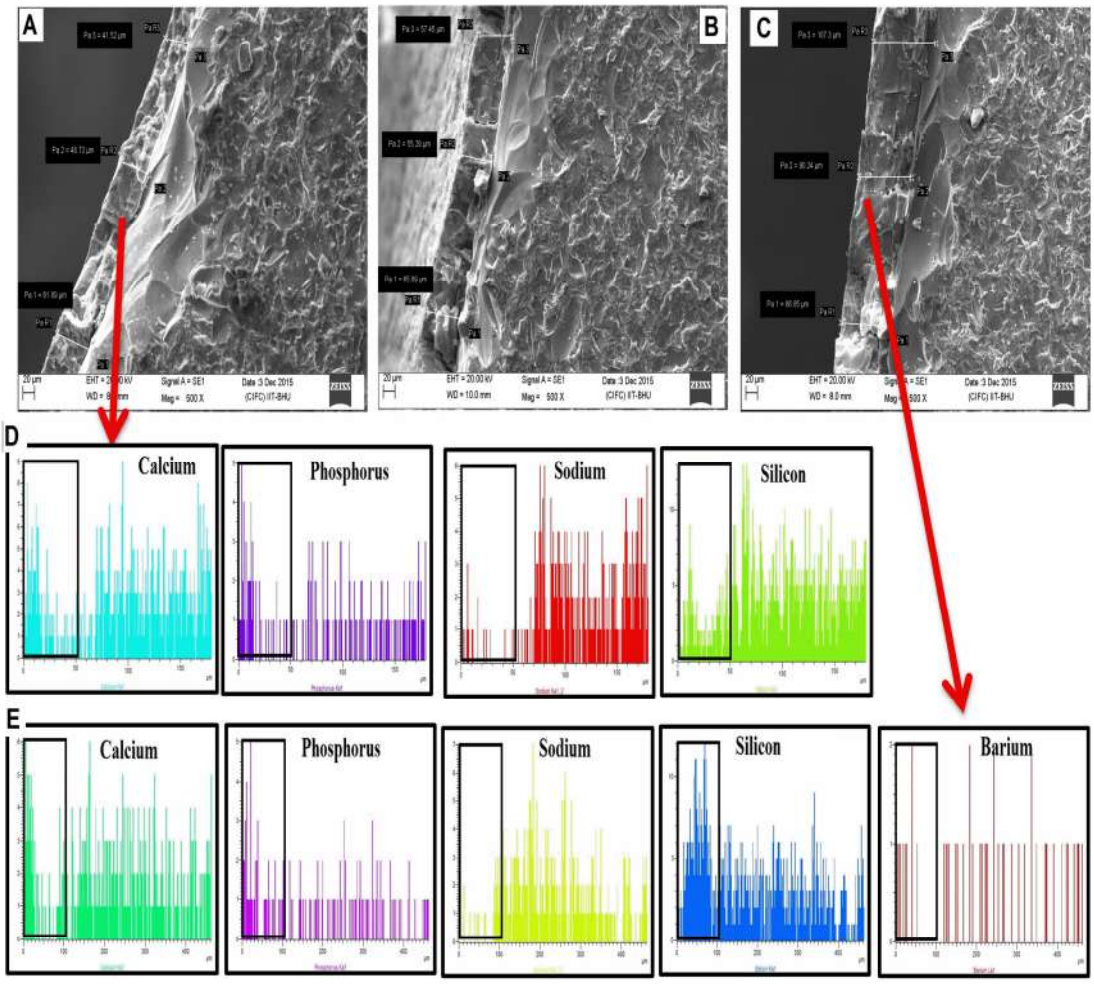

Figure 4.14 (A-C) HCA layer formation on the surface of the Ba-0, Ba-3 and Ba-4 bioactive glasses after immersion in SBF for 14 days, respectively, elemental mapping on (D) Ba-0 and (E) Ba-4 bioactive glasses

4.3.5 Physico -mechanical properties

A. Density of bioactive glasses

Figure 4.15 shows the variation of densities of bioactive glasses with BaO/SiO_2 ratio in the glass samples (Ba-0, Ba-1, Ba-2, Ba-3 and Ba-4). It is observed that the

densities of the samples were found to increase with increasing barium content in the glass from 2.70 to 2.81 gm/cm^3. It may be due to partial replacement of SiO_2 with BaO which is attributed due to the replacement of a smaller ion (Si^{4+}) with a bigger (Ba^{2+}) ion in the glass. In other words the lighter molar mass of SiO_2 (60.08 g/mol)) has been replaced by the heavier BaO (153.3 g/mol) in the bioactive glass samples.

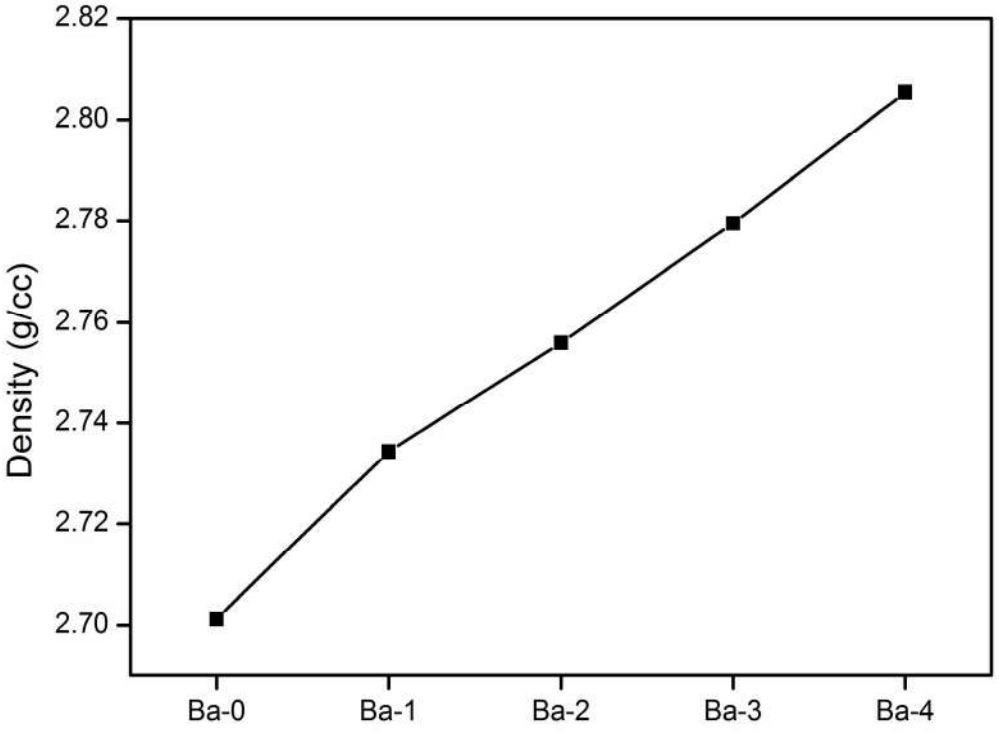

Figure 4.15 The variation in density with varying the BaO content in the bioactive glasses (Ba-0, Ba-1, Ba-2, Ba-3 and Ba-4)

B. Compressive strength of bioactive glasses

The mechanical stability of implant biomaterials is essentially required for repair of large bone defects to resist the mechanical stress caused during the clinical surgery and from implantation to complete conversion of HA [111]. The present study reports the mechanical properties with two different methods, namely destructive (compressive and flexural strength) and non-destructive (Young's modulus, bulk

modulus and shear modulus) tests for better understanding and conclusions of the samples. The bulk glass samples were cut, ground and polished to get optically. Five samples from each group were taken for test and the mean as well as standard deviation were calculated. The compressive strength results of the bioactive glasses are shown in **Figure 4.16**. It was observed that the compressive strength increased with increasing BaO concentration in the bioactive glass. The reason for the superior strength might be associated with the partial substitution of larger Ba^{2+} (atomic radius 2.22Å) ion at the cost of smaller Si^{4+} (1.11Å) ion in the glass network. It means that the presence of larger Ba^{2+} ion in the system increases the interference of the glass network. Therefore, the reduction in interatomic spacing results in the close packing of atoms [27][112]. This supports the observations well that the densities of the glasses were found to increase considerably with increasing concentration of BaO (**Figure 4.15**). Therefore, the packing density of the bioactive glass increases with barium addition. Thus, the increase in density of the bioactive glasses confirms an increase in compactness and densification, which could have resulted in an increase in compressive strength. Therefore, these results suggest that the substitution of baria in the bioactive glass increases the compressive strength significantly as compared with barium free bioactive glass (Ba-0).

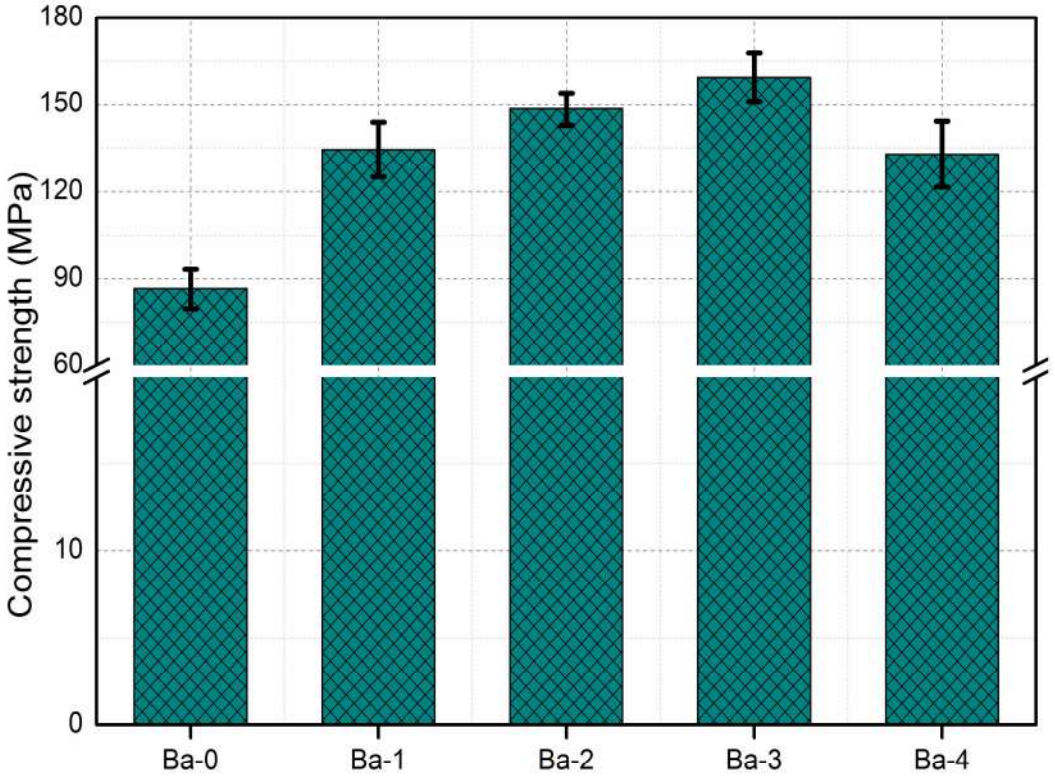

Figure 4.16 Compressive strength of the Ba-0, Ba-1, Ba-2, Ba-3 and Ba-4 bioactive glass samples

C. Flexural strength of bioactive glasses

Figure 17 shows the flexural strength of bioactive glasses determined to investigate the effect of barium substitution on the mechanical properties by change in BaO/SiO_2 ratio in the Ba-0, Ba-1, Ba-2, Ba-3 and Ba-4 bioactive glass samples. The flexural strength of the samples was found to increase with increasing barium concentration in the base glass from 47.38 to 65.39 MPa. On substitution of barium for silica in the composition acts as sintering additive which facilitated for early melting with more homogeneity in the glass, this would make the glass more rigid. The another main reason for the superior fracture strength can be explained by the Ba^{2+} ion which possesses a larger ionic radius than the Si^{4+} ion which occupies in interstitial

positions in the glass and makes the structure more dense in the glass network [43]. This might have resulted in higher mechanical properties. It can be clearly seen that the result of Ba-4 sample possessed highest mechanical strength as compared to Ba-0 sample this might be due to the presence of barium oxide only in the glass composition at the cost of SiO_2.

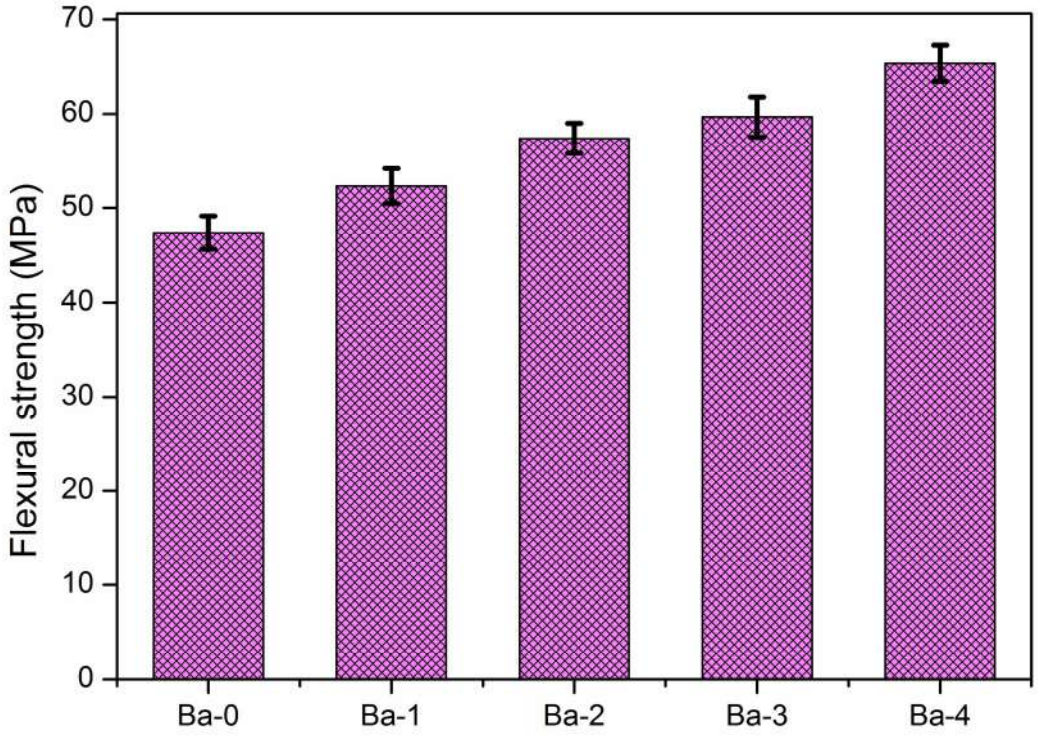

Figure 4.17 Flexural strength of the Ba-0, Ba-1, Ba-2, Ba-3 and Ba-4 bioactive glass samples

D. Modulus of elasticity

Young's modulus (E), shear modulus (S) and bulk modulus (K) of the bioactive glasses (Ba-0, Ba-1, Ba-2, Ba-3 and Ba-4) have been presented in **Table 2**. It was noticed that the Young's, shear and bulk moduli (elastic moduli) of the bioactive glass had increased with increasing BaO concentration in the glass. The elastic moduli of the bioactive glass increased linearly with increasing BaO content. These results are

comparable with the results of compressive strength. The improvement in elastic modulus of Ba-contained bioactive glass as compared with Ba-free sample could be due to the presence of larger Ba^{2+} ions in glass network. Further, it is to mention that the modifiers like Mg^{2+}, Ca^{2+}, Sr^{2+}, Ba^{2+} ions and etc. occupy the interstitial positions in the silicate network [40,98,99,112–116]. Therefore, the number of network bonds per unit volume increases in the glass structure. Hence, the propagation of sound wave in a compacted glass can be much quicker which results in the improvement in longitudinal and shear wave velocities and thus increase in elastic modulus. Further, It was also observed from earlier studies [99,114] that the glasses containing high amount of modifiers had shown better mechanical strength. Similarly, the gradual addition of BaO increases the modifier concentration in the glass which could have revealed a significant increase in elastic moduli of the bioactive glass.

Table 4.3 Young's modulus (E), shear modulus (S) and bulk modulus (K) of the Ba-1, Ba-2, Ba-3 and Ba-4)bioactive glasses

Sample No.	Young's modulus (E) (GPa)	Bulk modulus (K) (GPa)	Shear modulus (S) (GPa)	Network Connectivity (NC)
Ba-0	77.94 ± 7.11	40.60 ± 12.66	32.92 ± 0.57	2.12
Ba-1	80.91 ± 1.29	53.41 ± 4.25	32.45 ± 0.18	2.05
Ba-2	83.74 ± 3.19	54.59 ± 4.50	33.68 ± 1.41	1.99
Ba-3	84.91 ±0.47	51.05 ± 0.33	33.48 ± 0.19	1.94
Ba-4	85.81 ± 4.12	58.16 ± 4.86	34.26 ± 2.01	1.86

4.3.6 Cell culture studies

A. Effect of bioactive glasses on cell viability, proliferation and cytotoxicity

The *in vitro* cell culture studies were carried out using human osteosarcoma U2OS cell lines and assessed the cell viability, cytotoxicity, proliferation and attachment. In general, most of the biomaterials at lower concentrations can exhibit biocompatibility during cell culture studies. Therefore, at different concentrations and prolonged time period experimental models would provide the better evidences of the role of ions substituted in the glass. The cell viability of the samples (Ba-0, Ba-1, Ba-2, Ba-3 and Ba-4) was assessed using U2OS cell lines by XTT viability assay.

Figure 4.18 (A) shows the percent cell viability of the samples incubated for longer durations (18, 36 and 72 h) with a concentration of 25 mg/ml at 37^{o}C in 5% CO_2. The percent viability was calculated by considering the viability of tumor cell cultured in complete medium only as 100%. The results demonstrate that the barium contained bioactive glasses do not affect the viability of U2-OS cells in long term interaction in comparison to barium free sample (Ba-0). The U2-OS cells remain viable after co-culture with Ba-contained bioactive glasses (25 mg/ml) for 72 hours ($p>0.05$) and the cells were alive **(Figure 4.18 A)**. It was observed that the U2-OS cells remained healthy similar to that of untreated control cells following treatment with Ba-contained bioactive glasses. It is interesting to note that the Ba-4 sample contains high amount of barium (1.6 mol%) had demonstrated significant cell viability even after incubation at 72 h and this can be comparable with standard bioactive glass (Ba-0) sample. It was reported by earlier workers that the release of ions from the glass surface play an important role in cell survival [53,92,117]. Therefore, the release of ions from barium contained bioactive glasses does not harm the cell lines.

Cell proliferation assay was carried out at various concentrations (5, 10, 20, 50 and 100 mg/ml) of the bioactive glass samples incubated for 48 h as shown in **Figure 4.18 (B)**. The glasses containing barium did not inhibit the proliferation of U2-OS cells at all the concentrations studied in present investigation. A slight reduction in cell proliferation was recorded at the highest concentration (100mg/ml) although it remains insignificant corresponding to the control sample. The cell viability and proliferation data suggests that the substitution of barium in bioactive glass is tolerant to U2-OS cells with no significant loss of cell viability and proliferative capability. It was also reflected in the studies of direct cytotoxicity using different concentrations (5, 10, 20, 50 and 100 mg/ml) of bioactive glasses against U2-OS cells. The non-radioactive cytotoxicity assay demonstrates that all the samples have been found to be non-toxic. However, the sample Ba-4 exhibits slight toxicity at higher concentration (100mg/ml) although that remained non significant in comparison to barium free bioglass sample (Ba-0) as shown in **Figure 4.18 (C**). In quantitative analysis, as the concentration (mg/ml) of the glass sample increases in culture medium the toxicity increases due to greater sample to culture medium ratio, which might have caused cell death. Still the results of Ba-contained bioactive glasses are comparable with that of Ba-free one (Ba-0).

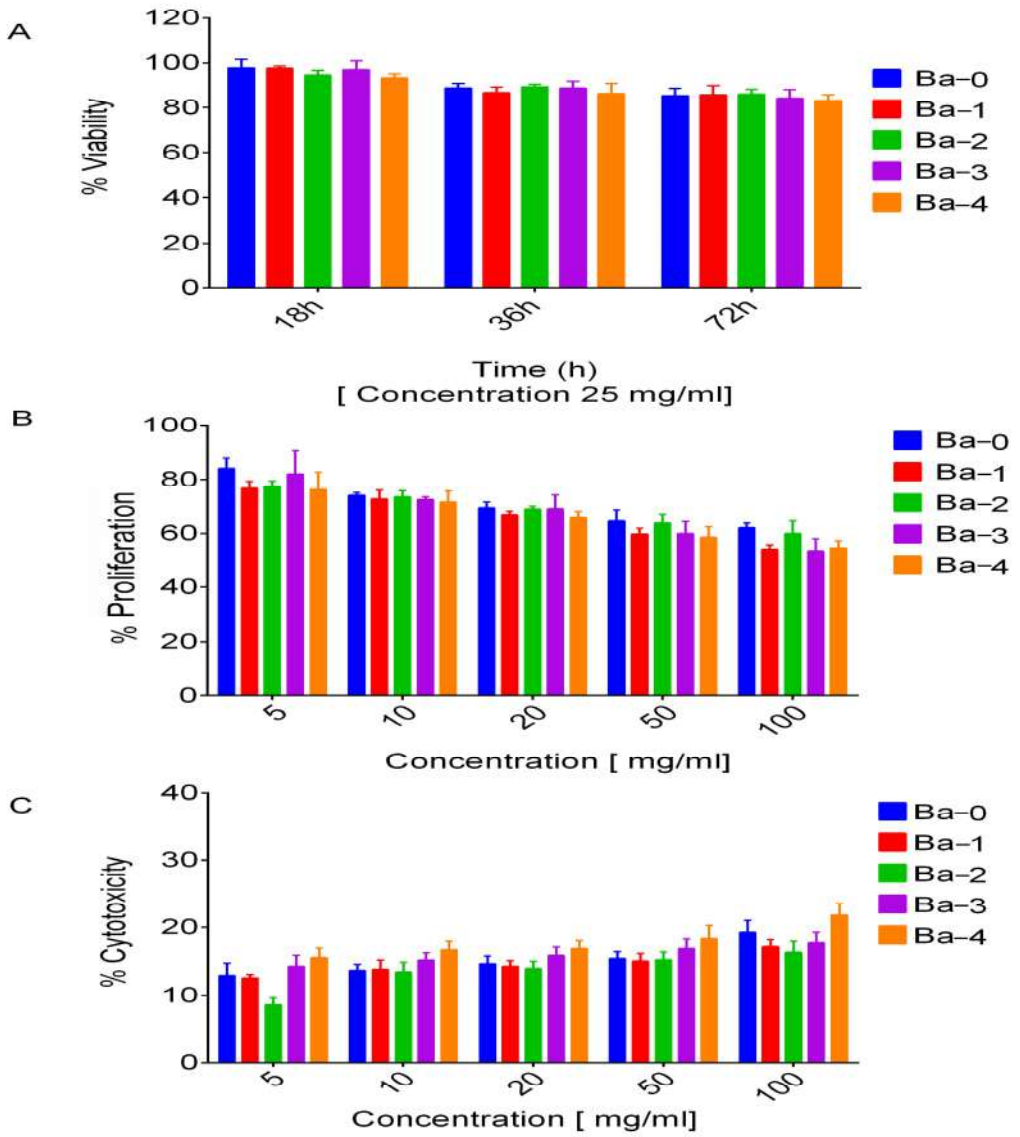

Figure 4.18 (A) Cell viability, (B) growth inhibition and (C) cytotoxicity of the Ba-0, Ba-1, Ba-2, Ba-3 and Ba-4.

B. Detection of cell apoptosis

It may be one of the reasons to consider that the cell inhibitory activity by the samples sometimes may cause cell death [78]. Therefore, we have also performed the cell apoptosis assay in the presence of the Ba-0, Ba-1, Ba-2, Ba-3 and Ba-4 bioactive glass samples. The apoptosis of cell was determined by monitoring the changes in the

cell size and externalization of phosphatidylserine of the U2OS cells. The fluorescence images represent the cell morphology treated with the bioactive glass samples are shown in **Figure 4.19**. The images demonstrate insignificant cell apoptosis by all the samples and apparently caused no harm to the U2-OS cells. Hence, these data further strengthen the observations that the presence of barium in the BG does cause cell apoptosis.

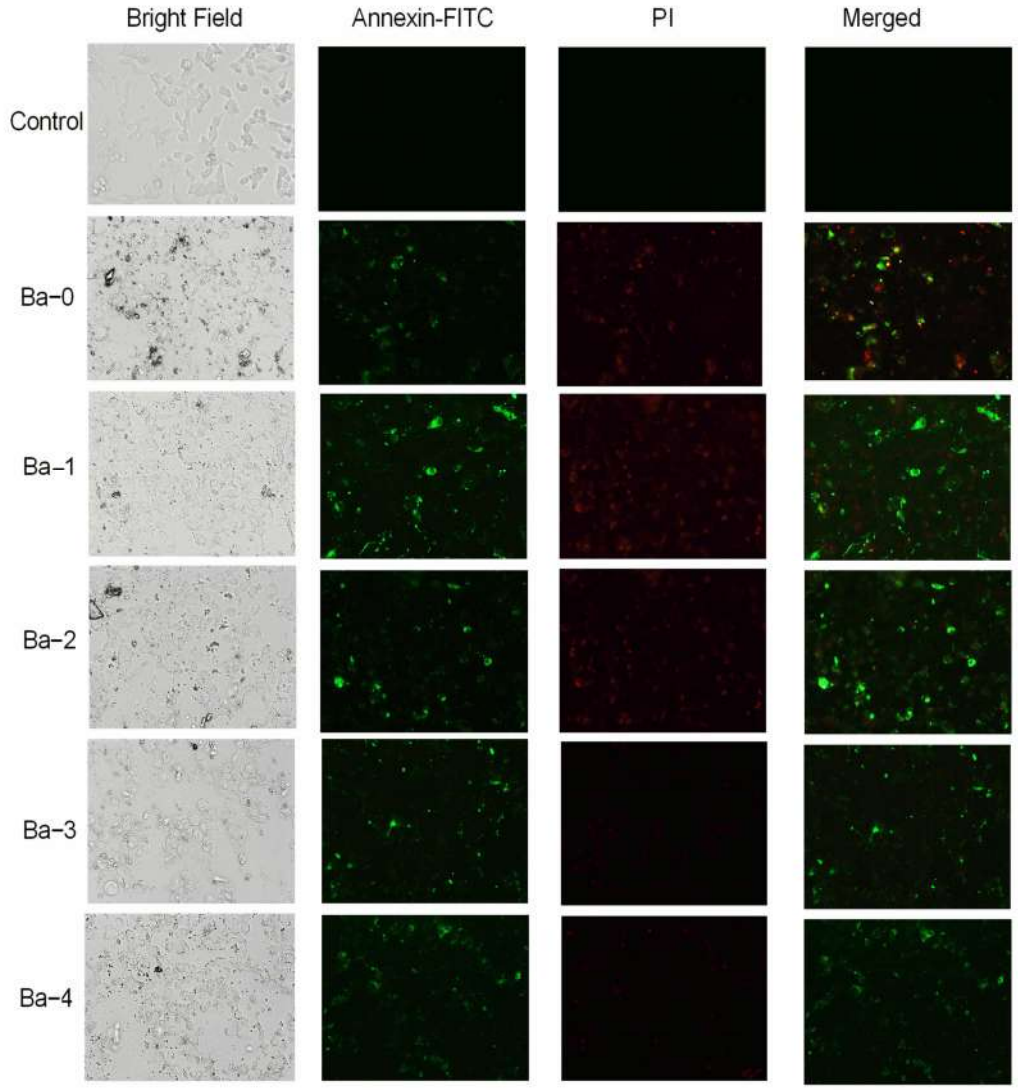

Figure 4.19 Microscopic analysis of induction of apoptosis. U2-OS cells were given indicated treatment with bioactive glass samples at a concentration of 5.0 μM, in complete RPMI 1640 medium for 8 h at 37 °C. The FITC-conjugated Annexin V and

Propidium iodide (PI) stained apoptotic cells were visualized under a fluorescence microscope (Nikon Eclipse 80i, Nikon, Japan) with Plan Fluor, 40×, NA 0.75 objective equipped with green and red filters for FITC and PI, respectively. n=4.

4.3.7 Cell attachment and growth on bioactive glasses

A. Live cell attachment and growth by light microscopic study

The *in vitro* osteoconductivity of osteosarcoma cells on the bioactive glasses have been evaluated in terms of cell adhesion and growth. We have cultured the U2-OS cells on the glass blocks in order to check the cell interaction with the glass samples and attachment on their surfaces. The U2-OS cells were found to grow on the surface of the blocks of bioactive glasses in 24 well plates in complete medium. The light microscope live images were taken at interface of the plate and BG blocks to differentiate between the adhesion and the growth of osteoblast-like cells. The cells were grown on the plate surface and were also found to grow over the BG blocks in 2 days following culture as shown in **Figure 4.20 (A-F)**. Gradually, the cells started growing and adhering significantly on all the BG blocks following continuous culture for 7 days as presented in **Figure 4.21 (A-F)**. The morphologies of the cells were changed apparently and the adhesive area was increased significantly with the incubation time. This growth could be attributed due to osteogenic differentiation by binding to its receptors directly on the surface of the osteoblast like cells. Therefore, the bone is continuously remodeling in a dynamic process where cell differentiation takes an active role for bone formation and this effect could be seen more on the Ba-contained BGs.

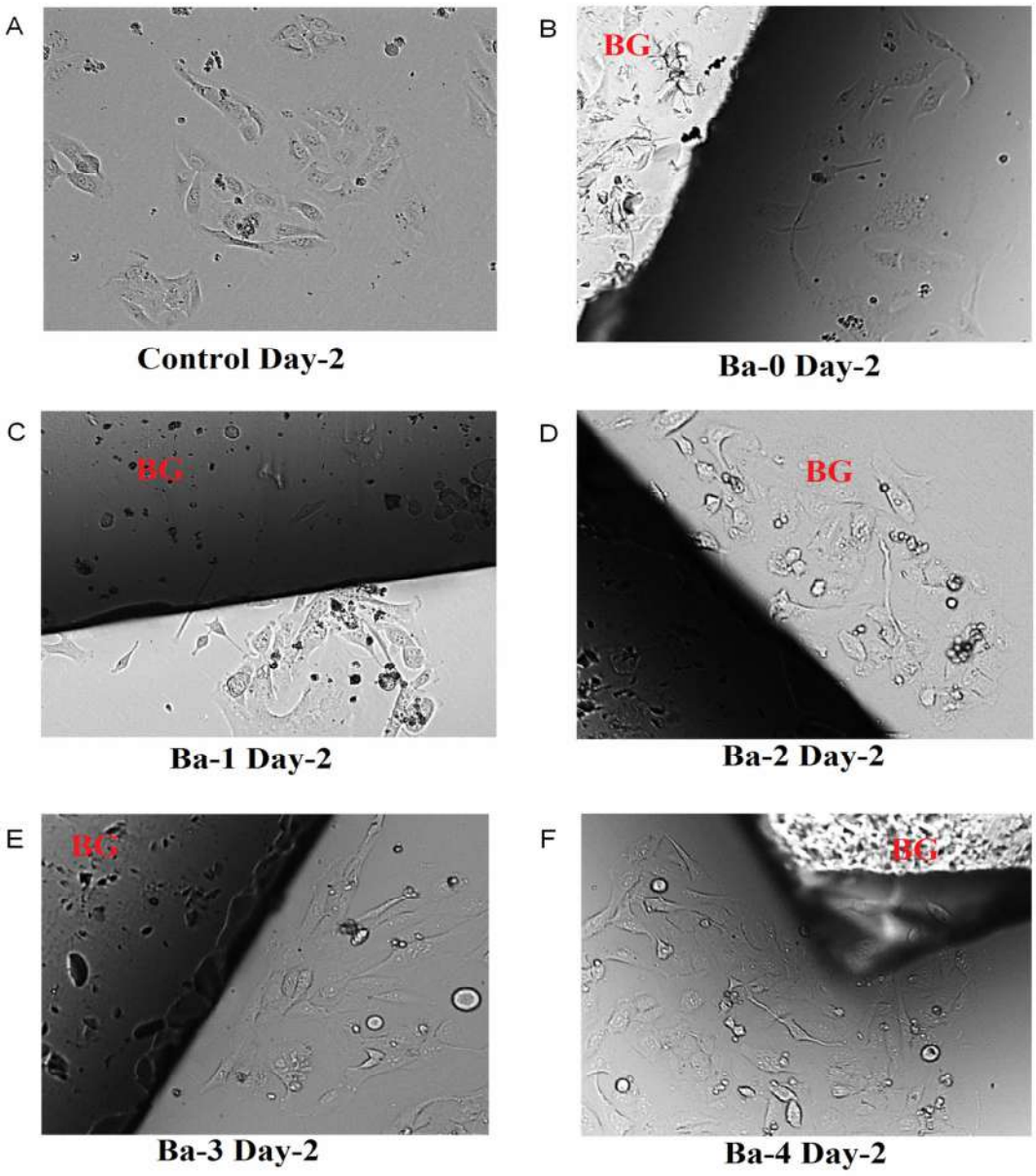

Figure 4.20 (A-F) Microscopic images of growth of U2-OS cells on bioactive glass blocks of control, Ba-0, Ba-1, Ba-2, Ba-3 and Ba-4 after 2 days of culture at 37 ^{o}C with 5% CO_2. U2-OS cells were grown in complete medium over the bioglasses in 24 well plates. Images were taken using inverted microscope (Nikon). n=2. BG written on the images represent the sample.

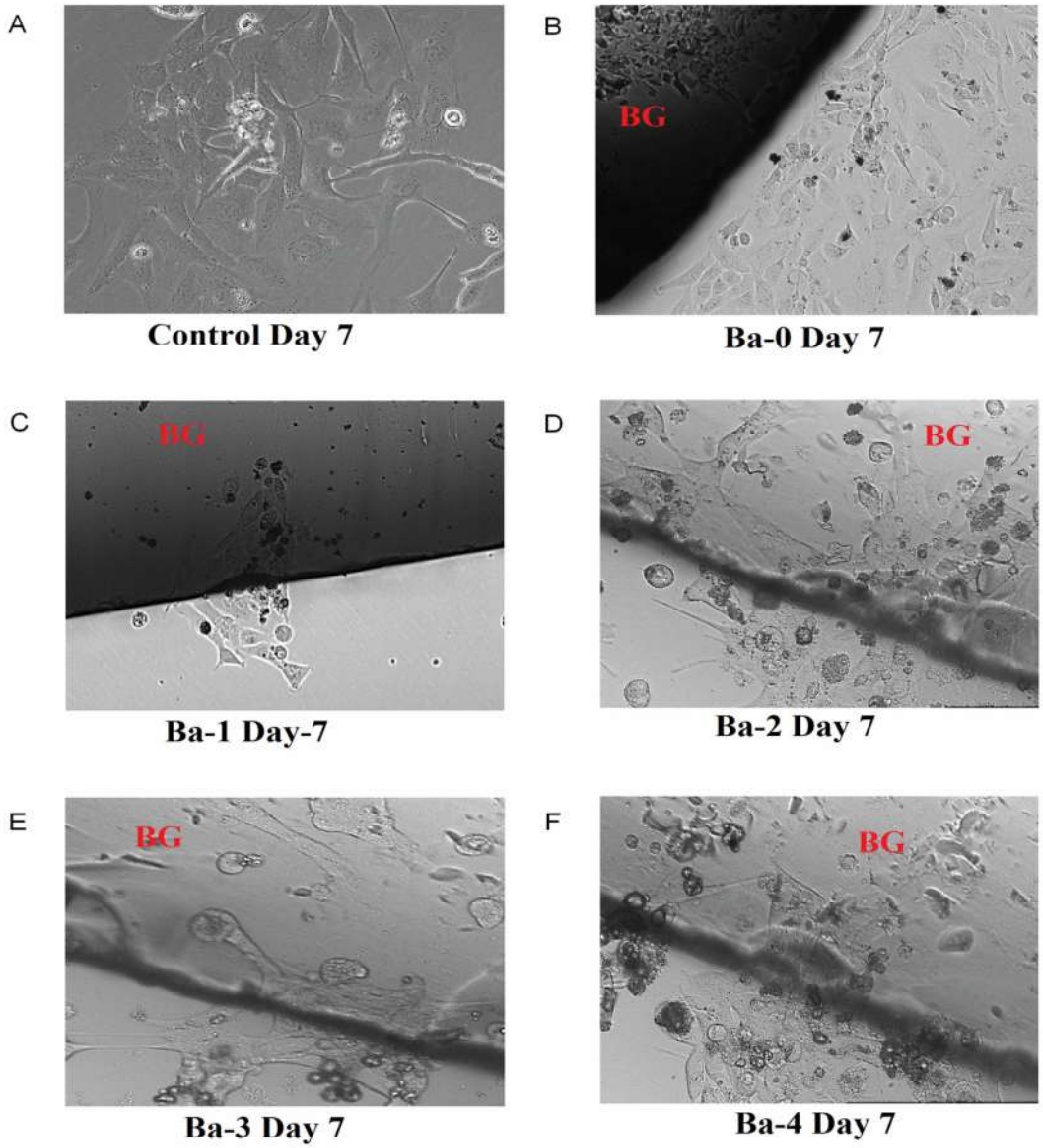

Figure 4.21 (A-F) Microscopic images of growth of U2-OS cells on bioactive glass blocks of control, Ba-0, Ba-1, Ba-2, Ba-3 and Ba-4 after 7 days of culture at 37 ^{o}C with 5% CO_2. BG written on the images represent the sample.

B. SEM & EDS analysis

Furthermore, the BG blocks were taken out from the culture plate and washed with PBS to remove the unattached cells and then the samples were dried and examined with SEM. The SEM images exhibit the bone mineralization and growth on Ba-0 and

Ba-3 as shown in **Figure 4.22 (A-B)** respectively. Ba-contained BG had shown significant growth of bone crystals as compared with Ba-free one. Further, the EDS analysis was also performed to assess the composition of the crystals on the surface of the Ba-0 and Ba-3 samples as shown in **Figure 4.22 (C-D)** respectively. The EDS spectra show the existence of Na, Ca, Ba, P and Si elements, while Ca and P are apparently high in amounts in comparison to other elements and this confirms the bone (Ca-P) layer formation on the surface of the samples. However, the reference sample (Ba-0) shows high amount of calcium deposition indicating the formation of calcite layer which is in good conformity with XRD data of the sample Ba-0 after immersion in SBF demonstrated a calcite layer formation (**Figure 4.12**). Further, the elemental mapping was also performed on the surface of the newly formed layer of Ba-3 sample (**Figure 4.23**). It was observed from Ba-3 sample that the presence of Ca and P ions were more in contrast in comparison to other ions (Si & Na) and these Ca and P ions were evenly distributed on the surface of the sample. This is further strengthening that the surface is rich in HCA layer formation. Further, it is interesting to note that the Ba^{2+} ions were found not only in the newly developed crystals but also on the entire surface of the Ba-3 sample as confirmed by EDS and mapping data shown in **Figures 4.22 (D) & 4.23** respectively. It might be due to the precipitation of Ba^{2+} ions in the HA matrix. This is in good support with the elemental distribution of SBF treated sample (Ba-4) which showed the presence of barium on the surface (**Figure 4.14**). Therefore, it is a good evidence and conformance from both the experiments (SBF treated and cell cultured) which had shown the presence of Ba^{2+} ions in the newly formed layer and hence barium is partially substituting in HCA to form the Ba contained HCA layer.

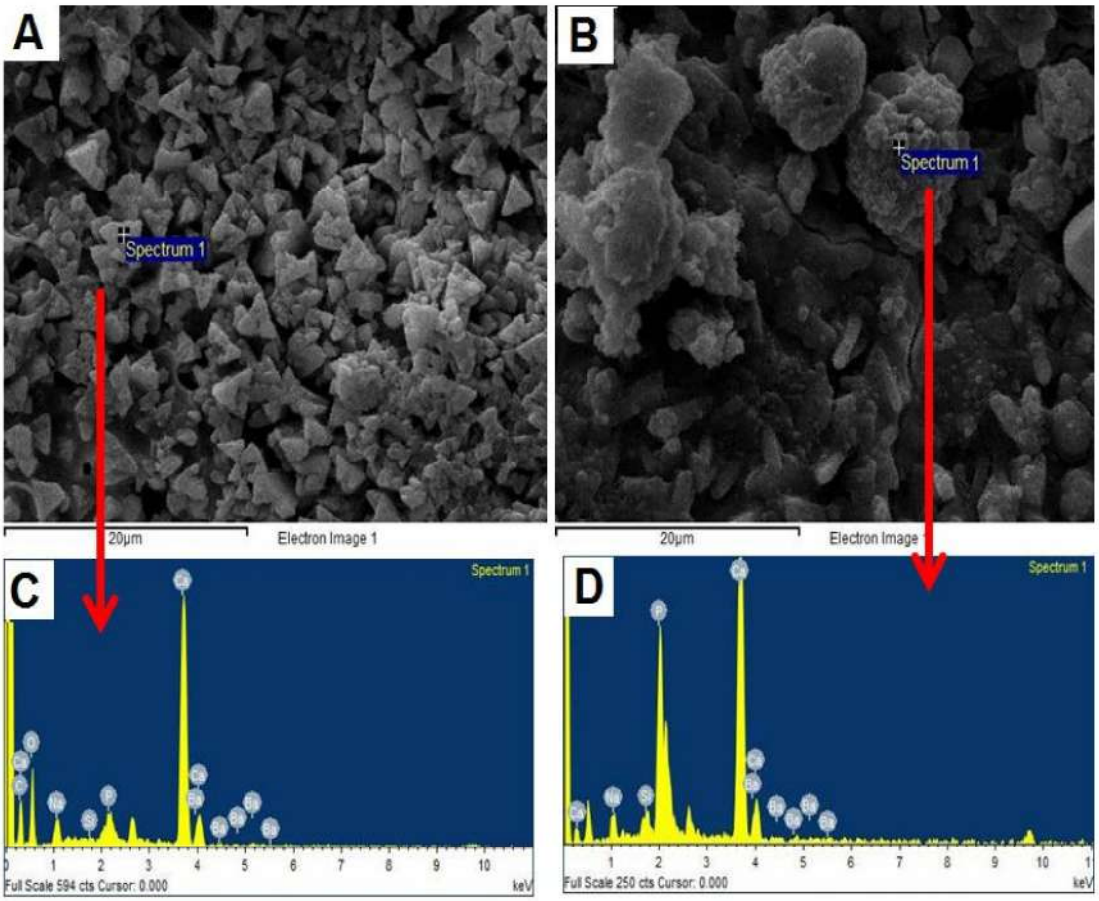

Figure 4.22 Cell attachment and growth on the bioactive glass blocks of Ba-0 (A) and Ba-3 (B) and their EDS analysis Ba-0 (C) and Ba-3(D), respectively

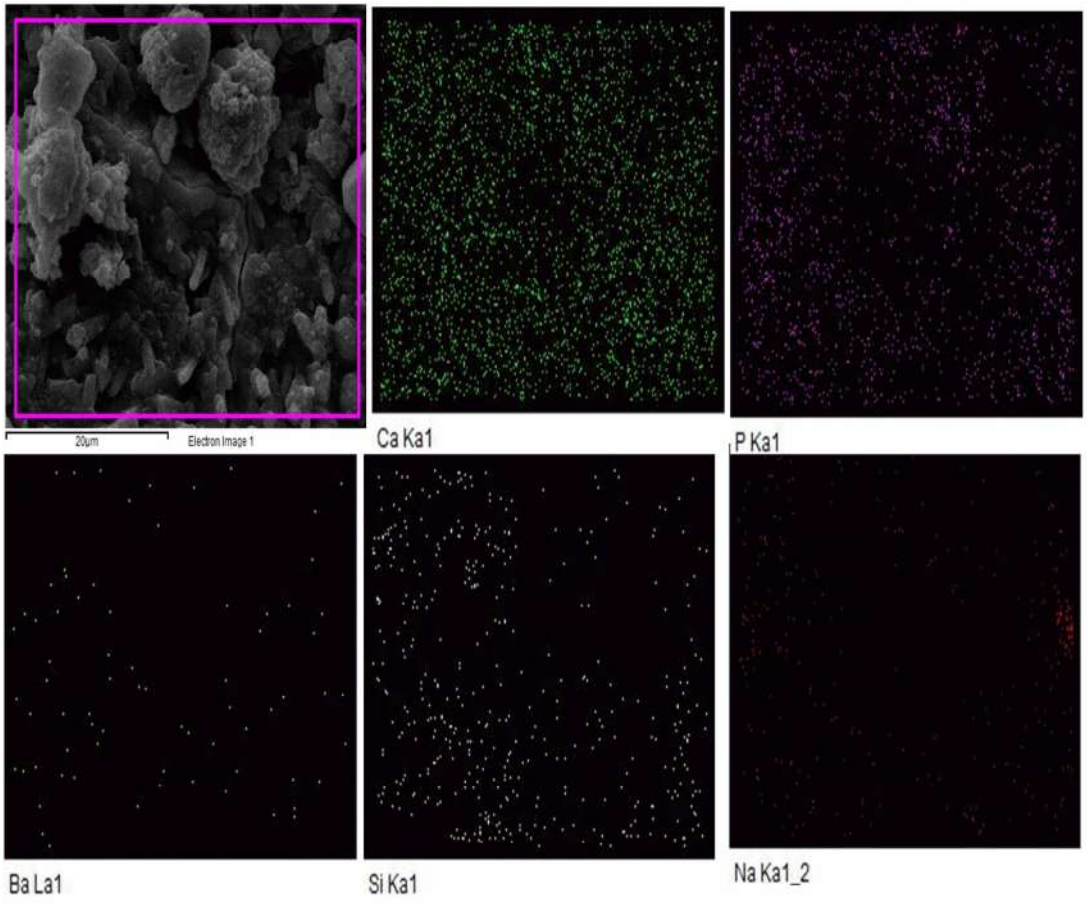

Figure 4.23 Elemental mapping on Ba-3 bioactive glass sample after cell culture for 5 days representing the presence of Ca, P, Ba, Si and Na ions

C. AFM analysis

Cell deposition and thickness formation on the glasses were assessed by AFM technique and it can be clearly seen from AFM (5µm X 5µm scanning area) topographic images that the bone mineralization and growth on the Ba-0, Ba-3 and Ba-4 bioactive glasses were present as in **Figure 4.24 (A-C)**, respectively. It was observed that the height profile of the samples increased significantly with increasing the Ba^{2+} ion concentration from 100 nm to 600 nm for Ba-0 and Ba-4 as shown in **Figure 4.24 (D-F)**, respectively. This might be due to the deposition of larger Ba^{2+} ions in the HA matrix and subsequent cell growth on the surface of the sample which is in

good conformity with thickness layer formed on the surface of the samples after immersion in SBF (**Figure 4.14)**. Yamaguchi et al. had demonstrated earlier that the barium can enter also into osteoblast like cells [45]. Thus, it is possible that barium might have entered into the HA matrix and resulted in an increase in height profile of the cell deposition (HCA layer). Moreover, the substitution of BaO for SiO_2 not only decreases the NC of the glasses but also decreases the surface charge. The surface charge also plays an important role in cell recruitment and growth, when lower is the surface charge higher would be the attachment [118]. Hence, the Ba-contained bioactive glasses might have recruited more number of cells on the surface of the sample which has resulted in an increase in height profile.

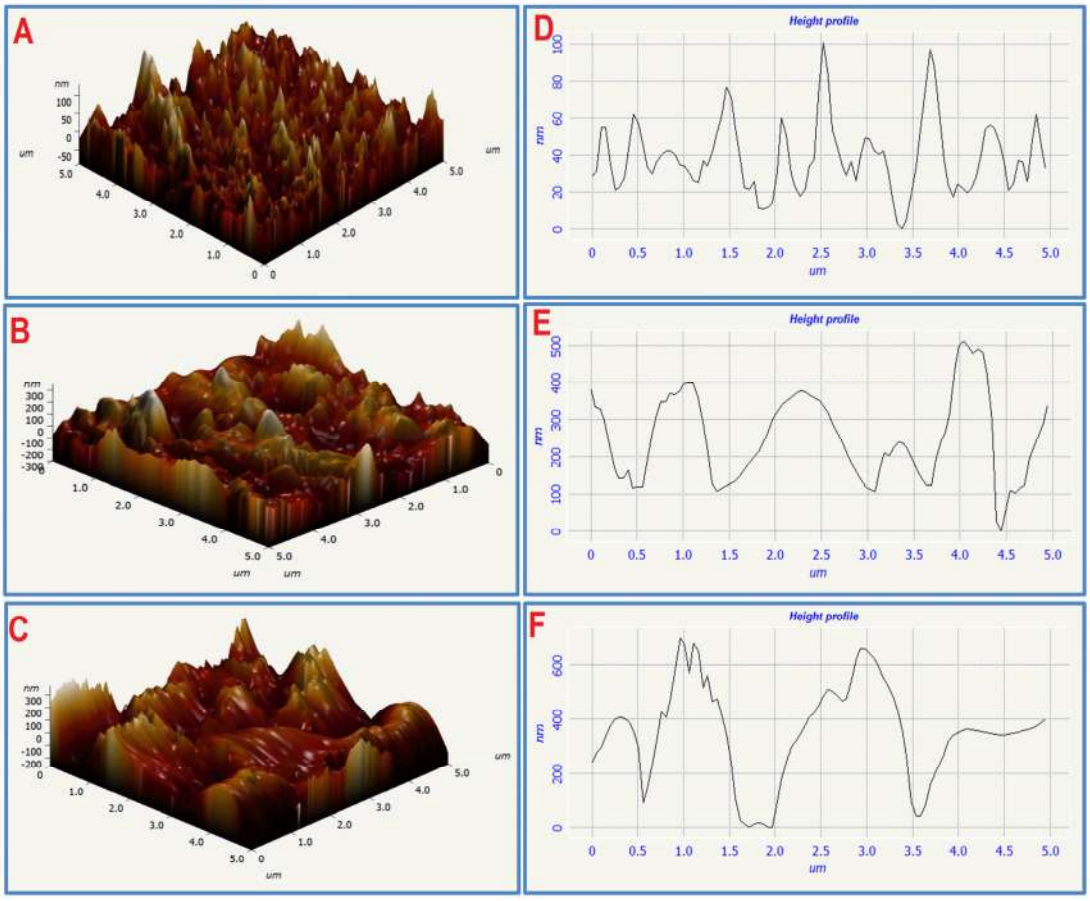

Figure 4.24 (A-C) AFM images of cell deposition on the Ba-0, Ba-3 and Ba-4 bioactive glass samples, respectively and (D-F) their height profile, respectively

4.3.8 Human blood compatibility assessment

A. Hemolysis, WBC viability, RBC integrity and size distribution

The *in vitro* blood compatibility of the bioactive glasses (Ba-0, Ba-1, Ba-2, Ba-3 and Ba-4) was assessed by hemolysis assay. Hemolysis takes place when the red blood cells (RBC) come in contact with the materials and it is important to verify the biomaterials before their *in-vivo* clinical trials. The hemolysis experiment has been carried out by culturing the samples with whole blood for longer duration of time (0.3 min, 1, 2 and 4 h). The % hemolysis caused by the bioactive glass samples (Ba-0, Ba-1, Ba-2, Ba-3 and Ba-4) were presented in **Figure 4.25 (A)** and it was found that it never exceeds 2.0% following time dependent study at a fixed concentration (20 mg/ml). These results are well within the limits (less than 5% according to ASTM F756-13) [119] even after 4 h in contact with blood. Thus, the substitution of barium in the bioactive glass is tolerant to the RBC and could be considered as non-hemolytic. This could also be seen in microscopic observations which exhibit no change in morphology of red blood cells (RBC) following in contact with the bioactive glasses (**Figure 4.25 C**). Further, it is noteworthy that the sample, Ba-4 shows lower hemolysis in comparison to other samples and hence the amount of barium in the BG seems to be compatible with blood. Furthermore, fresh peripheral blood mononuclear cell (PBMC) from normal donor was taken and examined the effect of these bioglasses on the PBMCs. It was observed that the PBMCs also remained unaffected by the Ba-contained bioactive glasses as compared with base glass after incubation for 18 h as shown in **Figure 4.25 (B)**. It can be clearly seen from the figure that there was no significant loss in viability even at higher concentrations and these results are comparable with the 45S5 bioglass® (Ba-0) **(Figure 4.25 B)**. Therefore, the results have shown that the

amount of barium in the BGs is compatible with blood white blood cells (WBC) and RBC as well as non hemolytic.

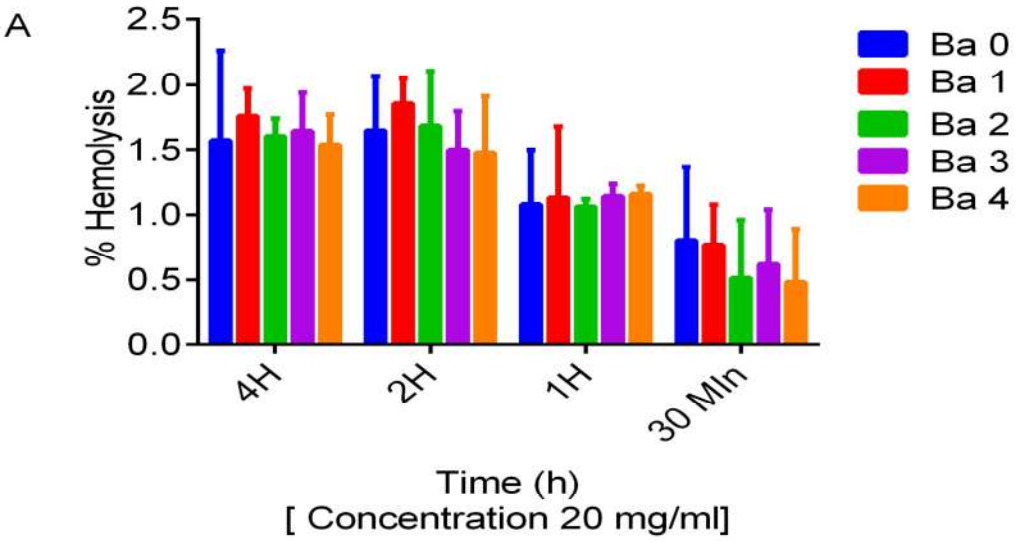

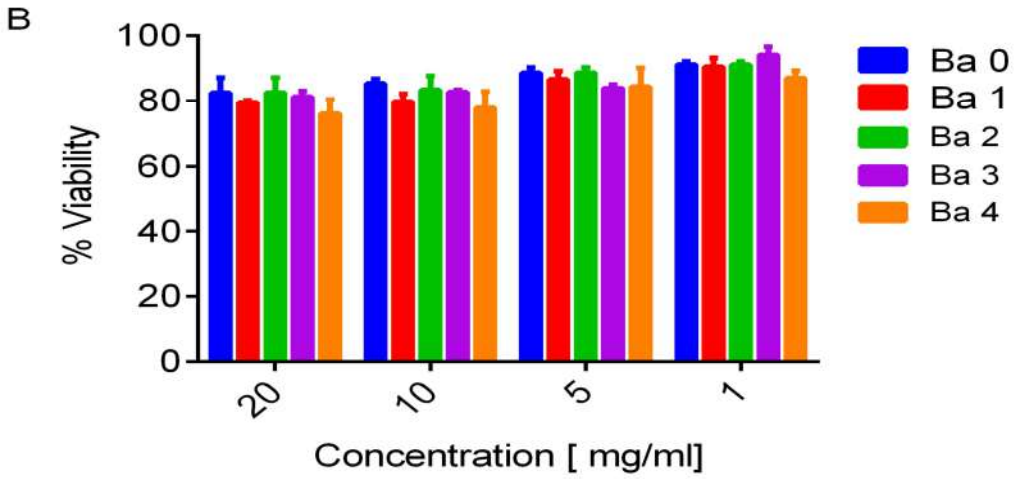

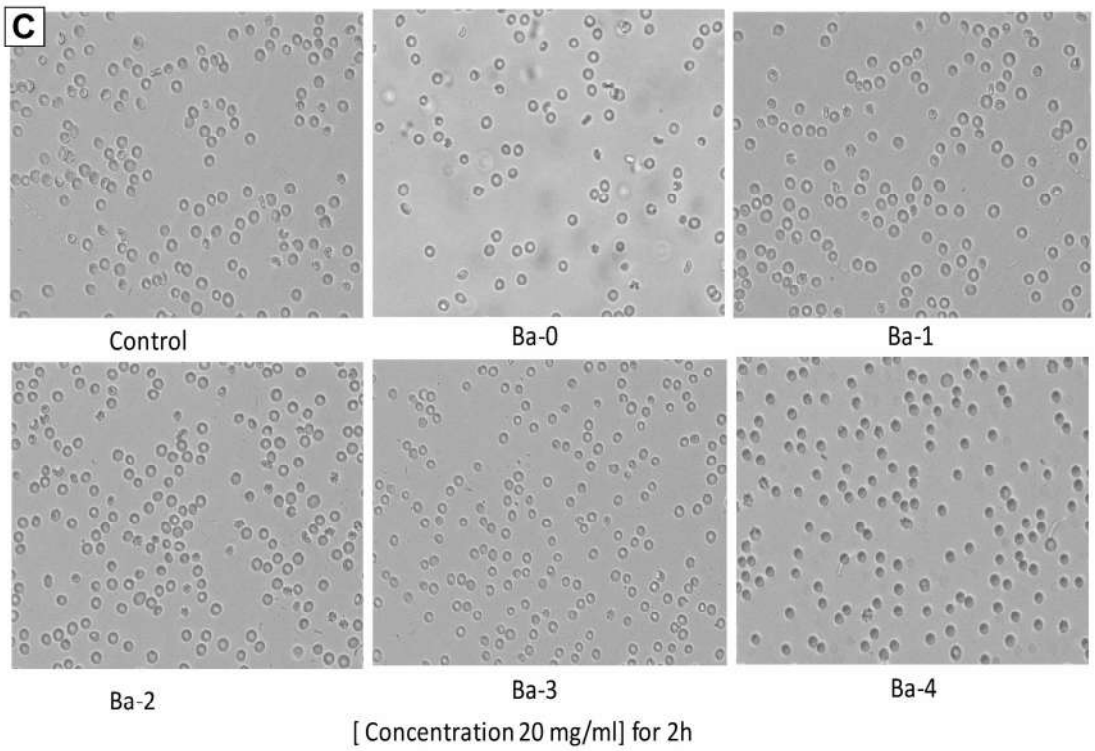

Figure 4.25 (A-C) Blood hemolysis induced in RBC by Ba-0, Ba-1, Ba-2, Ba-3 and Ba-4 bioactive glass samples with increasing time periods (A), Viability of PBMC in presence bioactive glasses at varying concentrations for 18 h and Mean ± SD, n=3 (B) and Photomicrographs demonstrate the effect of Ba-0, Ba-1, Ba-2, Ba-3 and Ba-4 bioactive glass samples on RBC morphology which was compared to untreated control (C).

B. Blood platelet aggregation and thrombus formation

It was seen from the pH study that the ions were released from the surfaces of the samples after immersion in SBF (**Figure 4.4**). Therefore, the amount of ions released from the sample might have entered into the human body fluids when implanted. This may cause sometimes platelet aggregation which involves blood coagulation due to the adhesion of platelets to fibrinogen, collagen and to implant surface and thus forms blood clots (thrombus formation). In order to examine the effect

of ions released from the sample on the platelets and its coagulation behavior, the supernatant of the SBF was taken out after immersion of the samples (Ba-0 and Ba-4) for 7 days and incubated with platelet rich plasma (PRP) ($2.5X10^8$ mL). **Figure 8.26** shows the change in % light transmittance with respect to time after incubation with PRP. It can be seen from the image that the sample Ba-0 has shown some platelet aggregation behavior after 8 min (95% change in light), whereas the sample Ba-3 has shown a lesser aggregation (88%). Therefore, the barium contained glasses can inhibit the blood coagulation and may not form the thrombus as compared with control.

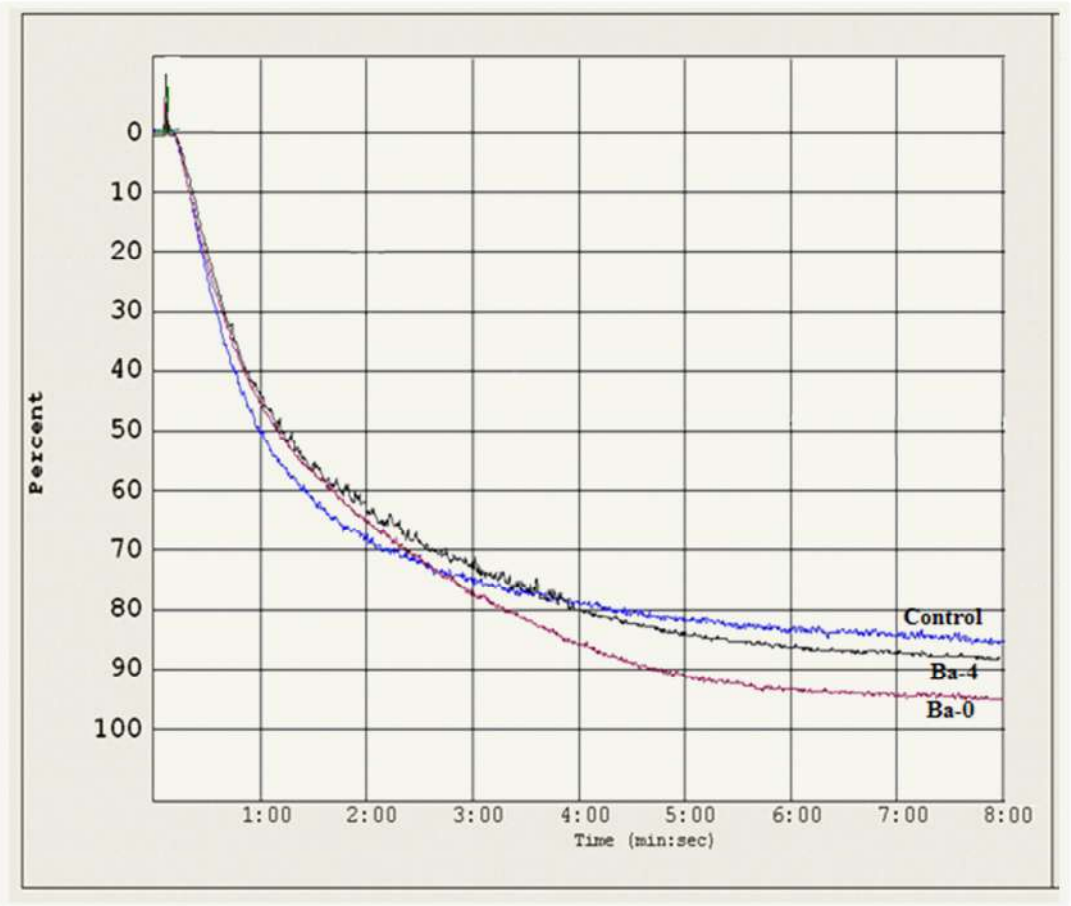

Figure 4.26 *In vitro* blood platelet aggregation behavior after incubation of supernatant of SBF of Ba-0 and Ba-4 samples with PRP for 8 min and the change in % light transmittance with respect to time (control is without sample)

4.3.9 Phagocytosis of bioactive glasses by human macrophage

In general, the bioactive glasses leach the ions when it is contact with the body fluids *in vitro* and *in vivo* and now it is important to study their phagocytosis behavior with human macrophages. In a typical bone transplantation scenario we could speculate that macrophages will be recruited in the areas of surgery in large numbers. These phagocyte cells take an active role in eating the foreign materials like bacteria, dead cells and unwanted pathogens in the human body. If the leached ions from the implant do not respond to the human macrophages then those ions will remain in the body which can cause adverse effect on the cells. Therefore, the phagocytosis behavior of Ba-0, Ba-1, Ba-2, Ba-3 and Ba-4 bioactive glasses with human macrophages was studied. Human macrophages were incubated with Ba-0, Ba-1, Ba-2, Ba-3 and Ba-4 bioactive glass samples (25 mg/ml) in complete medium for 24 h at 37 ^{o}C with 5% CO_2 and the percentage phagocytosis index is shown in **Figure 4.27**. It was observed that the ions released from the BGs were phagocytosed by the macrophages during incubation for 24 h. Moreover, the macrophages more active in scavenging the ions leached out from the Ba-containing BGs in comparison to Ba-free one. Moreover, it was reported that Mg^{2+} ion activates phagocytosis and regulates active calcium transport [120]. The barium also belongs to alkaline earth metal group like Mg^{2+}, Ca^{2+} and Sr^{2+} therefore; it may activate the phagocytosis and control the calcium transportation. It is in good conformance with XRD (**Figure 4.13**), SEM (**Figure 4.14**) and AFM (**Figure 4.24**) results in which the HCA layer found to increase with increasing barium content in the base bioglass® samples.

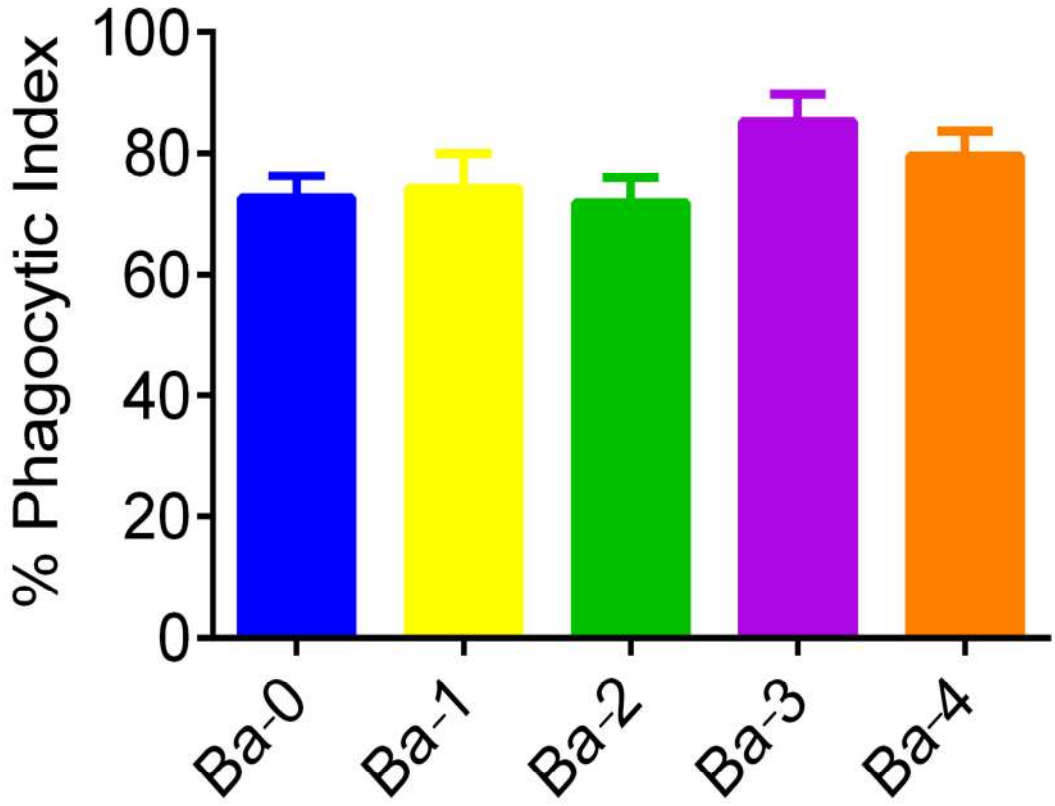

Figure 4.27 Human macrophages were cultured with Ba-0, Ba-1, Ba-2, Ba-3 and Ba-4 bioactive glasses in complete medium at 37 ^{o}C, 5% CO_2 for 24h. The cells were washed, fixed in ethanol and stained with Giemsa stain and observed under microscope. Intracellular particles were counted and percent phagocytosis was calculated for each treatment. Mean ±SD, n=3.

4.3.10 Opacity of the bioactive glasses by X-ray imaging

It has been demonstrated that the injection of radiopaque material is a simple technique for the treatment of osteoporotic bone or vertebral body fractures in spinal surgery [121]. The substitution of barium in BG not only increases the glass reactivity but also enhances the x-ray radiopacity of the bioactive glasses as shown in **Figure 4.28**. It can be clearly seen from the image that an increasing the barium concentration resulted in an increase in the radiopacity of the glass which is due to the presence of

radiopaque barium. Many authors have established that the addition of barium in bone cement ($BaSO_4$) increases its radiopacity which is very helpful during radiographic imaging. So that, one can identifies the cement location and precisely control depth of the cement in the bone during the clinical surgery. Moreover, the commercial bone cement (poly- methylmethacrylate, or PMMA) contains 10% barium [43][44]. Therefore, the substitution of barium in BG is useful and significantly enhances radiopacity which is very useful as a filling material in osteoporotic bone and dental applications.

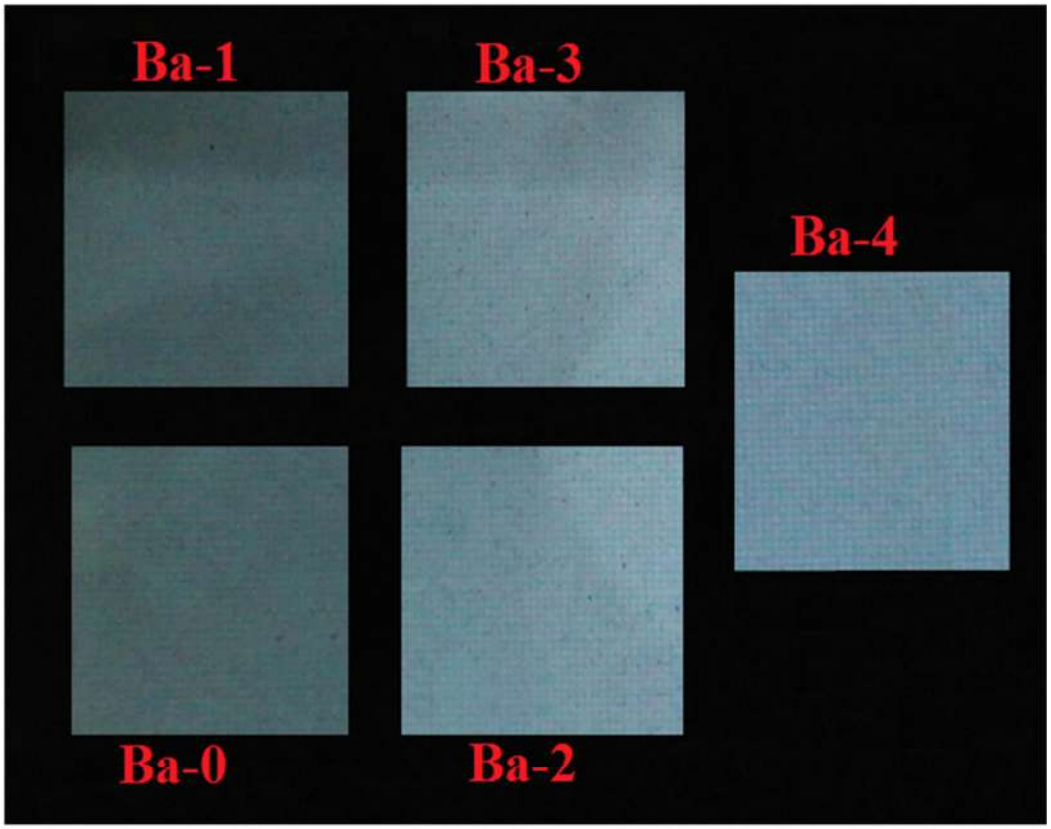

Figure 4.28 X-ray radiographic image of Ba-0, Ba-1, Ba-2, Ba-3 and Ba-4 bioactive glass samples

4.3.11 In vivo animal study

A. In vivo radiographic analysis

X-ray radiographic imaging is a primary and reliable diagnostic technique to examine the pre- and post-surgery status of bone fractures of the patients. The bioactive glasses (Ba-0 and Ba-3) have been filled in the drilled hole of rat femur bone as shown in photograph images (**Figure 4.29**). The X-ray radiographic images were taken for different time periods (0, 15, 30 and 45 days) after implantation of the samples Ba-0 and Ba-3 as shown in **Figure 4.30 (A-D)** and **(E-H)**, respectively. It can be clearly differentiated between the sample and the bone from radiographic images. However, the Ba-3 sample exhibits higher radiopacity in comparison to Ba-0 even during *in vivo* studies and it is in good conformity with the Ba-contained samples which had shown better radiopacity (**Figure 4.28**). This clearly suggests that one can easily identify the implant location and healing during *in vivo* evaluation. As the time increases the healing has taken place by both the samples after surgery. The hole filled with the Ba-0 sample shows some gap around this after 45 days of post implantation, where as Ba-3 sample completely healed after 45 days. This could be due to the enhanced bioactivity towards bone healing through cell growth on the surface of the sample. This is in good conformity with AFTM (**Figure 4.24**) images which demonstrated appreciable deposition of HCA layer on the surface of the samples.

Figure 4.29 Photographic images of *in vivo* implantation of bioactive glass sample in rat femur bone

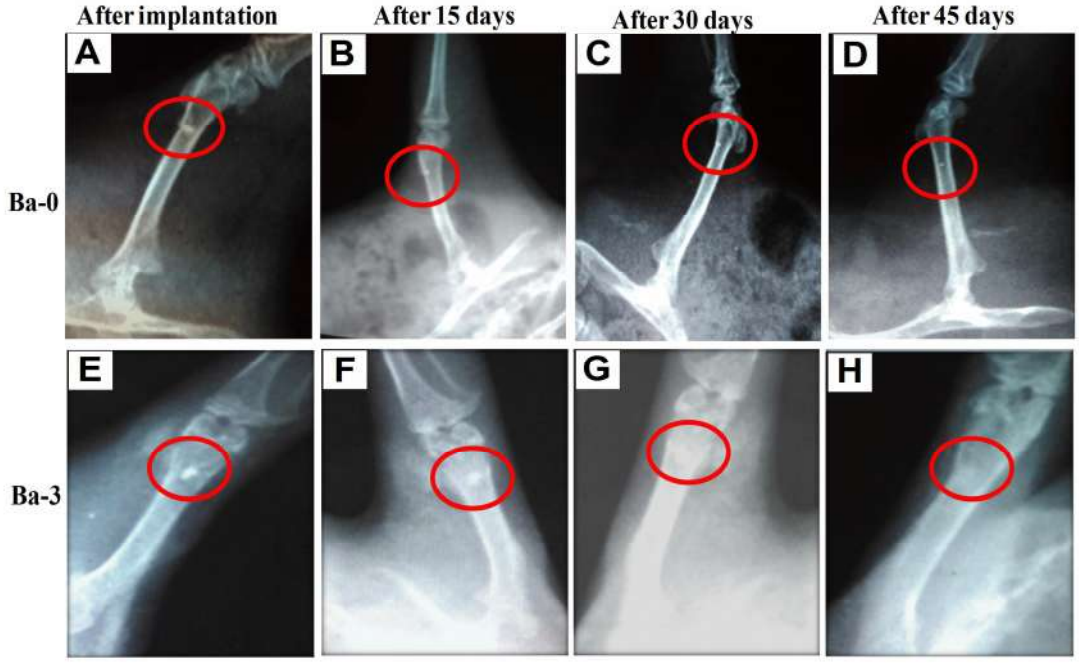

Figure 4.30 (A-D) X-ray radiograph images after implantation of Ba-0 sample for 0, 15, 30 and 45 days, respectively and (E-H) Ba-3 sample for 0, 15, 30 and 45 days, respectively in rat femur bone.

B. In vivo blood analysis

Figure 4.31 (A-H) shows the hematology analysis after surgery, the blood was drawn at different time periods such as 0, 10, 30 and 60 days post implantation of Ba-0 and Ba-3 samples. The blood was collected for complete blood count (CBC) such as red blood cell count (RBC), white blood cells (WBC), hematocrit, hemoglobin, mean corpuscular haemoglobin (MCH), mean corpuscular volume (MCV), mean corpuscular hemoglobin concentration (MCHC) and Platelet were studied. It was observed that, surgery leads to blood loss as a result of which on the 10^{th} day there was slight increase in the number of RBC which may be because of homeostasis in order to compensate the loss of RBC during the surgery **(Figure 31 B)**. As hemoglobin is the component of RBC and thus elevated level of RBC caused an increase in the count of hemoglobin on 10 day as shown in **Figure 31 (A)**. Platelet count increased on the initial days of surgery and it may be because of its tendency to activate cascade of pathways which helped in blood coagulation and normalized between 30 and 60 days as can be seen in **Figure 31 (D)**. Since white blood cells are associated with immunity and thus its level increased after surgery as recorded on 10^{th} day **Figure 31 (H)**. However, it normalized on 30^{th} and 60^{th} day. All the blood components reached to normal level on 60^{th} day of surgery as shown in **Figure 31 (A-H)**.

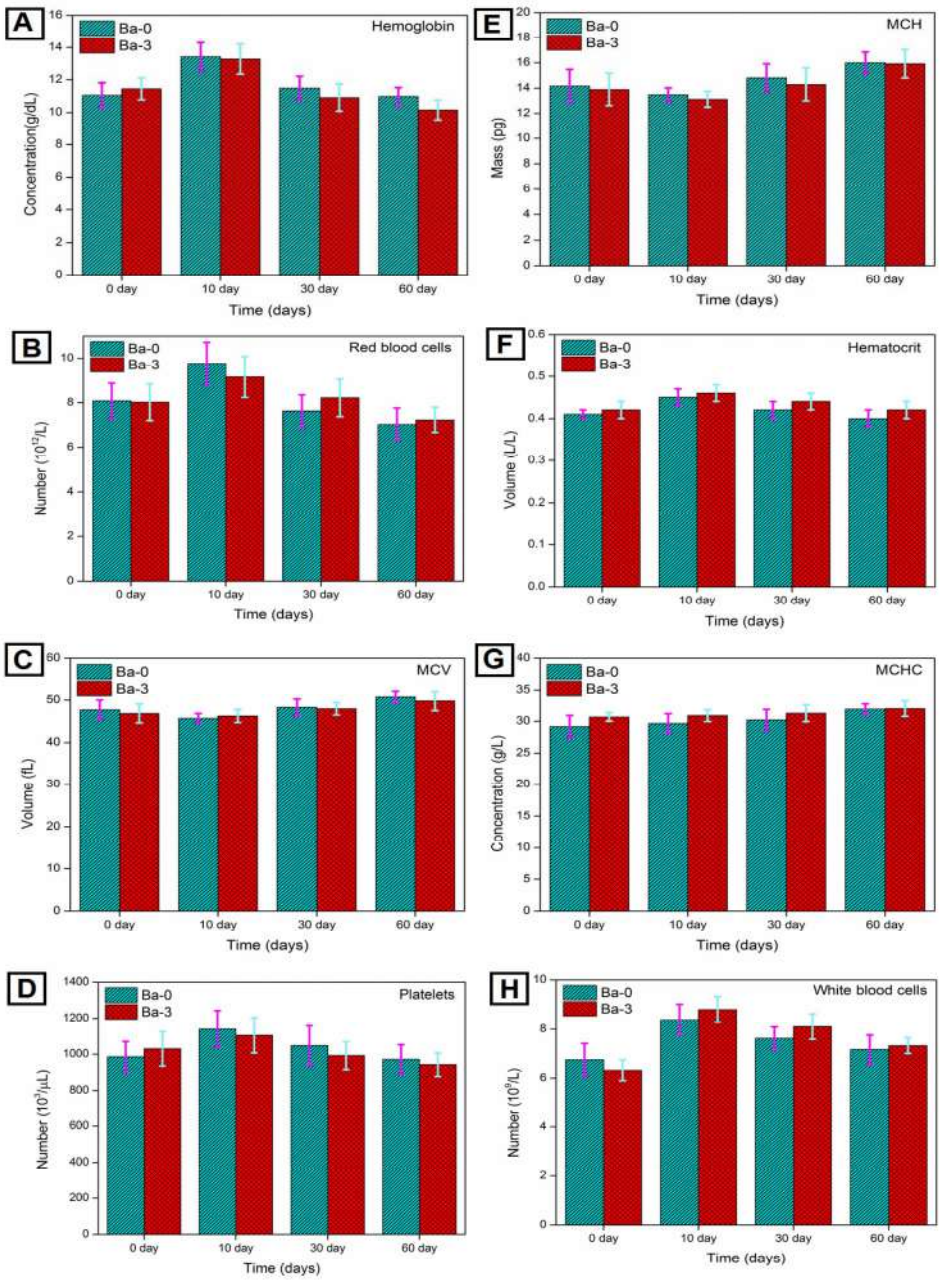

Figure 4.31 Hematology analysis after surgery at different time periods like 0, 10, 30 and 60 days. (A) Hemoglobin, (B) red blood cell count (RBC), (C) mean corpuscular volume (MCV), (D) Platelet, (E) mean corpuscular haemoglobin (MCH), (F) hematocrit, (G) mean corpuscular hemoglobin concentration (MCHC) and (H) white blood cells (WBC) and. Random blood sugar (RBS).

4.4 Conclusions

The main spirit of the research work is to enhance the properties of parent bioactive glass (45S5) without major alteration of the base glass composition. The bioactive glass system SiO_2–Na_2O–CaO–P_2O_5 was substituted with barium oxide in small quantities at the cost of silica and it has been successfully prepared. The bioactive glasses showed a decrease in glass nucleation and crystallization temperatures with increasing BaO content. Thermally treated base bioactive glass and barium substituted glasses have shown the main crystalline phases as $Na_2Ca_2Si_3O_9$. The XRD analysis of the bioactive glass before immersion in SBF revealed the amorphous nature of the glass. The FTIR spectrometry confirmed the presence of SiO_4 tetrahedra in the silicate glass network.

It has been demonstrated that the substitution of barium decreased the glass network connectivity and thus increased the glass dissolution which caused for the higher pH. The *in vitro* bioactivity in SBF had shown the formation of hydroxyl carbonate apatite layer on the surface of the base and barium contained bioactive glasses as confirmed by FTIR transmission spectrometry, pH behavior, XRD, SEM and EDS analysis. Moreover, the barium contained bioactive glass samples had shown superior bioactivity and higher HCA layer formation in comparison with reference to control sample. The density, compressive and flexural strengths were improved with an increase in BaO content in the base bioactive glass. Further, the Young's, bulk and shear modulus of the samples have also shown similar trends.

The *in vitro* cell culture studies like cell viability and cytotoxicity results have shown that the substitution of barium in the bioactive glass is compatible with human osteosarcoma U2OS cell lines and did not cause for cell apoptosis. It was also observed that the cells were proliferating. The U2OS cells were found to be significantly attached

and grown on the blocks of barium contained glasses as compared to control sample which was confirmed by SEM, EDS and AFM techniques.

Moreover the barium contained glasses have not caused for the blood hemolysis of RBC and they were also compatible with WBC. It was demonstrated that these glasses did not cause for blood platelet aggregation and hence do not form thrombus. It has been demonstrated that the amount of ions released from the glasses was phagocytosed by human macrophages but it was more prominent in barium contained bioactive glasses. Further, the substitution of barium has improved the radiopacity of the glasses which has a significant advantage during clinical surgery. The *in vivo* implantation of Ba-0 and Ba-3 samples in rat femur bone had exhibited the bone healing with increasing time but it was more active in barium contained BG as confirmed from X-ray radiographic images. The *in vivo* complete blood analysis (CBC) has also revealed that the base and barium contained BG did not affect on blood significantly. In view of the above results, the barium oxide can easily be substituted in base bioactive glass. The prepared barium contained bioactive glasses are promising for bone substitutes in biomedical applications.